III. MAPPING CRITICAL LEVELS FOR VEGETATION

Chapter 3 was prepared under the leadership of the ICP Vegetation* and led by Gina Mills, Head of the ICP Vegetation Programme Coordination Centre (PCC), Centre for Ecology & Hydrology, Bangor, UK, with support from the editorial team members Harry Harmens (Chair of the ICP Vegetation), Felicity Hayes (PCC), Håkan Pleijel (Chair Crops Working Group), Patrick Büker (Chair Forest Trees Working Group) and Ignacio González-Fernández (Chair (Semi-)natural Vegetation Working Group). Many other ozone experts from the ICP vegetation also contributed to the chapter, including Rocio Alonso, Jürgen Bender, Elke Bergmann, Viki Bermejo, Sabine Braun, Helena Danielsson, Giacomo Gerosa, Ludger Grünhage, Per Erik Karlsson and Riccardo Marzuoli, together with contributions from ICP Forests (Marcus Schaub) and EMEP (David Simpson).

This fully revised version of Chapter 3 includes updates to the critical levels for ozone agreed at the 30th ICP Vegetation Task Force Meeting, 14-17 February, 2017, Poznan, Poland. The critical levels for SO_2, NO_X and NH_3 and associated text have not been changed since the previous version. ***This version was published in April 2017 (minor edits October 2017).***

* International Cooperative Programme on Effects of Air Pollution on Natural Vegetation and Crops

Table of Contents

Note: in addition to this chapter, two additional scientific background documents (SBD) are available on the ICP Vegetation web site (http://icpvegetation.ceh.ac.uk):

- SBD-A: Supplementary material to Chapter 3 of Modelling and Mapping Manual;
- SBD-B: Developing areas and new directions of ozone research.

III. MAPPING CRITICAL LEVELS FOR VEGETATION

III.1 INTRODUCTION TO CRITICAL LEVELS FOR VEGETATION

The purpose of this chapter is to provide information on the critical levels of air pollutants for vegetation and the methodology for calculating critical level exceedance. Methods for mapping pollutant concentrations, deposition and exceedance are provided in Chapter II. The International Cooperative Programme on Effects of Air Pollution on Natural Vegetation and Crops (ICP Vegetation) has editorial responsibility for this chapter. Further information supporting the critical levels for ozone (O_3) and associated methodology can be found in the Chapter III Scientific Background Document A (SBD-A), whilst information on new developments in research for ozone critical levels is presented in the Chapter III Scientific background Document B (SBD-B), both available on the ICP Vegetation website (http://icpvegetation.ceh.ac.uk).

Excessive exposure to atmospheric pollutants has harmful effects on many types of vegetation and the ecosystem and food services that vegetation provides. Critical levels are described in different ways for different pollutants, including mean concentrations, cumulative exposures and cumulative uptake through small pores in leaves (stomatal flux). The effects vary between vegetation type or species and pollutant, and include changes in growth for trees and (semi-)natural vegetation, yield (quality and quantity) for crops, flower number and seed production for (semi-)natural vegetation, and vulnerability to abiotic stresses such as frost or drought and biotic stresses such as pests and diseases. Critical levels are defined as indicated in Box 1. Critical level exceedance maps show the difference between the critical level and the monitored or modelled air pollutant concentration, cumulative exposure or cumulative stomatal flux.

Box 1: Definition of critical levels for vegetation

Critical levels for vegetation are the "concentration, cumulative exposure or cumulative stomatal flux of atmospheric pollutants above which direct adverse effects on sensitive vegetation may occur according to present knowledge".

For **sulphur dioxide (SO_2)**, **nitrogen oxides (NO_x)** and **ammonia (NH_3)**, recommendations are made for concentration-based critical levels. For information on critical loads for sulphur and nitrogen acidity, and eutrophication due to nitrogen deposition see Chapter V. For **ozone (O_3)**, two types of critical levels are described for crops, forest trees and (semi-) natural vegetation: cumulative stomatal flux-based and cumulative concentration-based critical levels. Calculation of both incorporates the concept that the effects of O_3 are cumulative and values are summed over a specific threshold flux or concentration during daylight hours for a defined time period. As described in Section III.3.1, cumulative stomatal O_3 fluxes are considered biologically more relevant as they provide an estimate of the amount of O_3 entering the leaf pores and causing damage inside the plant (Mills et al., 2011a,b).

The critical levels have been set, reviewed and revised at a series of UNECE Workshops and ICP Vegetation Task Force Meetings, starting with Bad Harzburg (1988) and most recently in Madrid (2016) and at the 30th ICP Vegetation Task Force meeting in Poznan (2017); see Annex III.1 for a list of workshops. The critical levels for O_3 and associated methodology have been

primarily developed by the ICP Vegetation, with those for forests developed in collaboration with the ICP Forests (International Cooperative Programme on Assessment and Monitoring of Air Pollution Effects on Forests). Following agreement at ICP Vegetation Task Force Meetings or workshops, new or amended critical levels were subsequently put forward for approval at Task Force meetings of ICP Modelling and Mapping (International Cooperative Programme on Modelling and Mapping of Critical Levels and Loads and Air Pollution Effects, Risks and Trends), the joint meeting of the EMEP (The European Monitoring and Evaluation Programme) Steering Body and the WGE (Working Group on Effects) and the meeting of the Executive Body of the LRTAP Convention (http://www.unece.org/env/lrtap/welcome.html).

III.2 CRITICAL LEVELS FOR SULPHUR DIOXIDE (SO_2), NITROGEN OXIDES (NO_X) AND AMMONIA (NH_3)

III.2.1 SULPHUR DIOXIDE (SO_2)

The critical levels for SO_2 that were established in Egham in 1992 (Ashmore & Wilson, 1993) are still valid (Table III.1). There are critical levels for four categories of vegetation types – for sensitive groups of lichens, for forest ecosystems, (semi-)natural vegetation and for agricultural crops. These critical levels have been adopted by WHO (2000).

Exceedance of the critical level for (semi-)natural vegetation, forests, and, when appropriate, agricultural crops occurs when either the annual mean concentration or the winter half-year mean concentration is greater than the critical level; this is because of the greater impact of SO_2 under winter conditions.

***Table III.1**: Critical levels for SO_2 ($\mu g\ m^{-3}$) by vegetation category.*

Vegetation Type	Critical level SO_2 [$\mu g\ m^{-3}$]	Time period
Cyanobacterial lichens	10	Annual mean
Forest ecosystems*	20	Annual mean and Half-year mean (October-March)
(Semi-)natural	20	Annual mean and Half-year mean (October-March)
Agricultural crops	30	Annual mean and Half-year mean (October-March)

**The forest ecosystem includes the response of the understorey vegetation.*

III.2.2 NITROGEN OXIDES (NO_X)

The critical levels for NO_x are based on the sum of the NO and NO_2 concentrations because there is insufficient knowledge to establish separate critical levels for the two pollutants. Since the type of response varies from growth stimulation to toxicity depending on concentration, all effects were considered to be adverse. Growth stimulations were of greatest concern for (semi-)natural vegetation because of the likelihood of changes in interspecific competition.

Separate critical levels were not set for classes of vegetation because of the lack of available information. However, the following ranking of sensitivity was established:

(semi-)natural vegetation > forests > crops

Critical levels for NO_x were established in 1992 at the Egham workshop. The background papers on NO_x and NH_3 presented at the Egham workshop (Ashmore & Wilson, 1993) were further developed as the basis of the Air Quality Guidelines for Europe, published by the WHO in 2000. This further analysis incorporated a formal statistical model to identify concentrations to protect 95% of species at a 95% confidence level. In this re-analysis, growth stimulation was also considered as a potentially adverse ecological effect. Furthermore, a critical level based on 24h mean concentrations was considered to be more effective than one based on 4h mean concentrations as included in the earlier version of the Mapping Manual (UNECE, 1996). Since the WHO guidelines were largely based on analysis extending the background information presented at the Egham workshop, the critical levels in Table III.2, which are identical to those of WHO (2000), should now be used.

Table III.2: *Critical levels for NO_x (NO and NO_2 added, expressed as NO_2 ($\mu g\ m^{-3}$)).*

Vegetation Type	Critical level NO_x (expressed as NO_2) [$\mu g\ m^{-3}$]	Time period
All	30	Annual mean
All	75	24-hour mean

For application for mapping critical levels and their exceedance, it is strongly recommended that only the annual mean values are used, as mapped and modelled values of this parameter have much greater reliability, and the long-term effects of NO_x are thought to be more significant than the short-term effects.

Some biochemical changes may occur at concentrations lower than the critical levels, but there is presently insufficient evidence to interpret such effects in terms of critical levels.

III.2.3 AMMONIA (NH_3)

The fertilisation effect of NH_3 can in the longer term lead to a variety of adverse effects, including growth stimulation (which can alter species balance with some less sensitive species being potentially out-competed) and increased susceptibility to abiotic (drought, frost) and biotic stresses. In the short-term there are also direct effects. As for NO_x, for application for mapping critical levels and their exceedance, it is strongly recommended that only the annual mean values of NH_3 are used, as mapped and modelled values of this parameter have much greater reliability, and the long-term effects of NH_3 are thought to be more significant than the short-term effects.

The critical levels in Table III.3 refer to ecosystems with the most sensitive lichens and bryophytes and higher plants. The aim of the critical levels defined is to protect the functioning of plants and plant communities. Lichens and bryophyte species were found to be more sensitive than higher plants, while the critical levels given in Table III.3 for higher plants apply for native and forest species. Critical levels are not currently set for intensively managed agricultural grasslands (pastures) and arable crops, which are often sources rather than sinks of ammonia.

Table III.3: *Critical levels for NH_3 (µg m^{-3}).*

Vegetation type	**Critical level NH_3 [µg m^{-3}]**	**Time period**
Lichens and bryophytes (including ecosystems where lichens and bryophytes are a key part of ecosystem integrity)	1	Annual mean
Higher plants (including heathland, grassland and forest ground flora)	3*	Annual mean
Provisional critical level		
Higher plants	23	Monthly mean

**An explicit uncertainty range of 2-4 µg m^{-3} was set for higher plants (including heathland, semi-natural grassland and forest ground flora). The uncertainty range is intended to be useful when applying the critical level in different assessment contexts (e.g. precautionary approach or balance of evidence.)*

The critical levels presented in Table III.3 were recommended for inclusion in this manual at a workshop, held in Edinburgh from 4-6 December, 2006: *Atmospheric ammonia: Detecting emission changes and environmental impacts* (UNECE, 2007). Their inclusion was subsequently approved at the 20th Task Force meeting of the ICP Vegetation (Dubna, Russian Federation, 5-8 March, 2007) and adopted at the 23rd meeting of the Task Force on Modelling and Mapping (Sofia, Bulgaria, 26-27 April, 2007). The Edinburgh meeting (December, 2006) recommended the following:

1. A revision of the currently set values of the ammonia critical levels. The data reviewed show that the previous/existing critical level values of 3300 µg m^{-3} (hourly), 270 µg m^{-3} (daily), 23 µg m^{-3} (monthly) and 8 µg m^{-3} (annual) were not sufficiently precautionary;
2. A new long-term critical level for lichens and bryophytes, including ecosystems where lichens and bryophytes are a key part of the ecosystem integrity, of 1 µg m^{-3} (annual mean);
3. A new long-term critical level for higher plants, including heathland, grassland and forest ground flora and their habitats, of 3 µg m^{-3}, with an uncertainty range of 2-4 µg m^{-3} (annual mean);
4. The workshop noted that these new long-term critical level values are based on observation of actual species changes from both field surveys and long-term exposure experiments, where effects were related to measured ammonia concentrations. The workshop noted that the long-term critical levels could not be assumed to provide a protection for longer than 20-30 years;
5. To retain the monthly critical level (23 µg NH_3 m^{-3}) for higher plants only as a provisional value. This value is based on the assessment of adverse effects of short-term exposures as discussed at the UNECE workshop on Critical Levels held in 1992 in Egham, United Kingdom (Van der Eerden et al., 1993). The monthly critical level was estimated with the "envelope" method using exposure-response data from mainly short-term fumigation experiments. Thus, it has not the same relevance as the long-term critical levels (annual averages of 1 and 3 µg NH_3 m^{-3}) derived from long-term field studies. The provisionally retained monthly value has to be considered as expert judgement to allow the assessment of effects of short-term peak concentrations which can occur during periods of manure application (e.g. in spring).

The proceedings of the UNECE Workshop on Ammonia (Edinburgh, December 2006) were

published in Sutton et al. (2009) by Springer: Sutton M.A., Baker S., Reis S. (eds.), *Atmospheric Ammonia: Detecting emission changes and environmental impacts*. This book includes details of the evidence used to justify the change in critical levels.

In summary, the key evidence, which was based on observations of changes in species composition change (a true ecological endpoint) in response to measured air concentrations of ammonia, is provided in Table III.4.

Table III.4: *Summary of 'no-effect' concentrations (NOECs) of the impact of long-term exposure to NH_3 on species composition of lichens and bryophytes.*

Location	Vegetation type	Lowest measured NH_3 concentration [µg m^{-3}]	Estimated NOEC * [µg m^{-3}]	Reference
SE Scotland, poultry farm	Epiphytic lichens	0.6	0.7 (on twigs) 1.8 (on trunks)	(Pitcairn et al., 2004, Sutton et al., 2009)
Devon, SW England	Epiphytic lichens diversity (twig)	0.8 (modelled)	1.6	(Wolseley et al., 2006)
United Kingdom, national NH_3 network	Epiphytic lichens	0.1	1.0	(Leith et al., 2005, Sutton et al., 2009)
Switzerland	Lichen population index	1.9 (modelled)	2.4	(Rihm et al., 2009)
SE Scotland, field NH_3 experiment, Whim bog	Lichens and bryophytes – damage and death	0.5	< 4	(Sheppard et al., 2009)
Corroborative evidence **				
SW England	Epiphytic lichens	1.5	ca. 2	(Leith et al., 2005)
South Portugal	Epiphytic lichens	0.5	1	(Pinho et al., 2009)
Italy, pig farm	Epiphytic lichens	0.7	2.5	(Frati et al., 2007)

***NOECs were directly estimated from exposure/response curves or calculated with regression analysis. The data are from recent experimental studies, both field surveys and controlled field experiments on the impact of NH_3 on vegetation.*

***In these cases NH_3 concentration data were available for less than one year, which is why these results are categorised as "corroborative evidence".*

III.3 CRITICAL LEVELS FOR OZONE (O_3)

III.3.1 OVERVIEW

III.3.1.1 O_3 DAMAGE TO VEGETATION AND CONSEQUENCES FOR FOOD PRODUCTION AND ECOSYSTEM SERVICES

A large body of evidence has shown that ambient O_3 causes damage to O_3-sensitive vegetation. O_3 enters leaves via the stomatal pores on the leaf surface. Once inside the leaf, a series of chemical reactions occur leading to damage to cell membranes and other negative impacts on plant metabolism, including photosynthesis. These effects can be in response to short-term episodes or cumulative during the growing season, and can lead to:

- Visible leaf damage and premature aging of leaves;
- Reductions in above- and below-ground growth and biomass;
- Changes in the ratio between shoot and root biomass (including carbon allocation);
- Reductions in flower number, flower biomass and seed production;
- Reductions in crop yield quantity and quality, including cereal grains, potato tubers and tomato fruit;
- Changes in forage quantity and quality for pasture;
- Altered tolerance to abiotic stresses such as drought and frost and biotic stresses such as pest attacks and diseases.

Reviews of O_3 effects on vegetation have been published for crops (Ainsworth, 2016), trees (Matyssek et al., 2012, Wittig et al., 2009) and (semi-)natural vegetation (Bassin et al., 2007, Fuhrer et al., 2016), whilst effects on carbon sequestration are reviewed by Ainsworth et al. (2012). ICP Vegetation has published a series of reports on O_3 effects on vegetation, including food security (Mills & Harmens, 2011), carbon sequestration (Harmens & Mills, 2012), ecosystem services and biodiversity (Mills et al., 2013).

Widespread evidence of O_3 damage to vegetation in Europe was reported (Mills et al., 2011a) including visible leaf injury on crops, trees (Gottardini et al., 2016) and (semi-) natural vegetation, reductions in growth of O_3-sensitive compared to –resistant cultivars and biotypes, and beneficial effects on yield and growth of reducing the ambient O_3 concentration by filtration. O_3 effects have also been reported in the field in the USA (Fuhrer et al., 2016; Temple et al., 2005; U.S. Environmental Protection Agency, 2014) and south-east Asia (Emberson et al., 2009, Feng et al., 2015) and are present in other regions of the world (Fuhrer et al., 2016). Meta-analyses of published data have also indicated that ambient O_3 is reducing crop yield (Pleijel, 2011) and tree biomass production (Wittig et al., 2009), whilst analysis of survey data has shown how O_3 is reducing tree growth (Braun et al., 2014) and changing species composition, a biodiversity indicator (Payne et al., 2011).

The many impacts of O_3 have been considered when developing critical levels. **Here, we provide critical levels for the potential O_3 effects on:**

- Crop yield quantity and quality, for food security applications, including economic valuation;
- Tree biomass for timber production and potentially as a starting point for carbon sequestration and biodiversity application;
- Grassland biomass, potentially as a starting point for carbon sequestration and flower and seed production, potentially as a starting point for biodiversity application.

III.3.1.2 METRICS FOR CRITICAL LEVELS OF O_3 FOR VEGETATION

A glossary for all terms used for O_3 critical levels is provided in Annex III.2.

For O_3, two types of metrics are available for risk assessment, either based on the cumulative stomatal flux or the cumulative exposure. Scientific evidence suggests that observed effects of O_3 on vegetation **are more strongly related to the uptake of O_3**

through the stomatal leaf pores (stomatal flux) than to the concentration in the atmosphere around the plants (Mills et al., 2011b). Stomata are physiologically controlled and respond to environmental conditions such as temperature, light, air humidity and soil moisture, as well as plant growth stage. For example, under hot and dry conditions, plants close their stomata to reduce water loss and as a consequence O_3 uptake is reduced. The DO_3SE model (Deposition of O_3 for Stomatal Exchange) has been developed to account for the variation in stomatal opening and closing with climatic, soil and plant factors (Büker et al., 2012; Emberson et al., 2000a,b, 2001, 2007). This model, described in Section III.3.4.3, and available as an online version at: https://www.sei-international.org/do3se, is used to determine the Phytotoxic O_3 Dose above a threshold flux of Y (POD_Y) which is the accumulated stomatal O_3 uptake during a specified time period. Different metrics have been developed for POD_Y depending on the complexity of the model and its application, see Box 2 for definitions.

Box 2: Metrics for stomatal flux-based critical levels

POD_Y (Phytotoxic O_3 Dose) is the accumulated plant uptake (flux) of O_3 above a threshold of Y during a specified time or growth period.

POD_YSPEC is a species or group of species-specific POD_Y that requires comprehensive input data and is suitable for detailed risk assessment.

POD_YIAM is a vegetation-type specific POD_Y that requires less input data and is suitable for large-scale modelling, including integrated assessment modelling.

The flux-based POD_Y metrics are preferred in risk assessment over the concentration-based AOT40 exposure index (defined in Box 3). AOT40 accounts for the atmospheric O_3 concentration above the leaf surface and is therefore biologically less relevant for O_3 impact assessment than POD_Y as it does not take into account how O_3 uptake is affected by climate, soil and plant factors. This is particularly relevant on the pan-European scale with large climate differences between different regions. AOT40 can be used in cases where only O_3 concentration data are available (when meteorological and/or vegetation-specific information to calculate POD_Y are not available) and/or areas where no climatic or water restrictions to stomatal O_3 flux are expected. This approach predicts a different spatial pattern of impacts on the pan-European scale than POD_Y (Mills et al., 2011a; Simpson et al., 2007).

Box 3: Metric for concentration-based critical levels

AOT40 is the sum of the differences between the hourly mean O_3 concentration (in ppb) and a threshold value of 40 ppb O_3 when the concentration exceeds 40 ppb during daylight hours, accumulated over a stated time period.

Different types of evidence show that the relationships between effects and exposure are improved by consideration of the defence capacity of the plants, whereby a certain amount of absorbed O_3 is detoxified in the plants and does not impact on the overall effect (Mills et al., 2011b). This is variable by species and is accounted for by including an hourly cut-off Y flux in POD_Y and concentration X in AOT_X (with X being 40 ppb in AOT40).

III.3.1.3 ESTABLISHMENT OF CRITICAL LEVELS FOR O_3

The methods described in this chapter have been developed by:

- Combining data from available field studies to calibrate species-, vegetation type- and biogeographical region specific- models of leaf stomatal opening to quantify the stomatal O_3 flux for different plant species;
- Combining the results from available studies in Europe where plants were exposed to different levels of O_3 under field conditions to derive response functions from which critical levels are derived;
- Testing the critical levels using observations in the field under ambient conditions, wherever feasible.

Metric-response relationships have been established using experimental data from exposure systems such as open-top chambers that enable plants to be grown under naturally varying climatic conditions for one or more growing seasons. Data from several countries and years of experiments have been combined, wherever possible, for a single species/vegetation type. The approach described by Fuhrer (1994) for calculating relative effect (e.g. yield or biomass), now expressed as a percentage, has been used for each experimental dataset. The relative effect was obtained per data point by dividing the observed values of the response variables by the intercept of the linear regression between the response variable and O_3 exposure for each experiment (i.e. for a hypothetical cumulative stomatal flux or exposure equal to zero) and converted to percentage, to provide a relative effect for each data point. After this transformation, the data from all experiments were combined to derive a common response function for each species/vegetation type and effect. The 95% confidence intervals are shown on flux-effect relationships to give an indication of the strength of the relationship and the range of significance of effect for a given POD_Y (SPEC or IAM). Response functions used to derive the AOT40-based critical levels are provided in the scientific background document A (SBD-A).

In some circumstances when the POD_Y is being calculated, reference against a POD_Y of 0 could theoretically lead to a critical level that is not achievable as the O_3 concentrations needed to achieve this could be lower than the estimated “pre-industrial” O_3 concentration. Hence, at the O_3 Critical Level Workshop in Madrid in November 2016, it was decided that an accumulated flux value calculated at a constant 10 ppb O_3 (estimated pre-industrial mean O_3 concentration) should be set as a reference value (Ref10 POD_Y) for determining flux-based critical levels (SBD-A). Ref10 POD_Y was first determined for the same set of experimental data used for derivation of flux-effect relationships by calculating POD_Y using a constant O_3 concentration of 10 ppb and the climatic conditions in the experiment. If data from several experiments were combined from different climates, the mean of the Ref10 POD_Y was used as the Ref10 POD_Y for that function. The application of this approach in the derivation of a critical level is shown in Figure III.1. This approach is not needed for AOT40-based critical levels as the cut-off concentration of 40 ppb in calculating AOT40 is substantially higher than estimated pre-industrial O_3 concentration (SBD-A).

Each critical level was derived from a response function using a species or vegetation-specific percentage effect. The choice of percentage value for each critical level is explained in the separate sections.

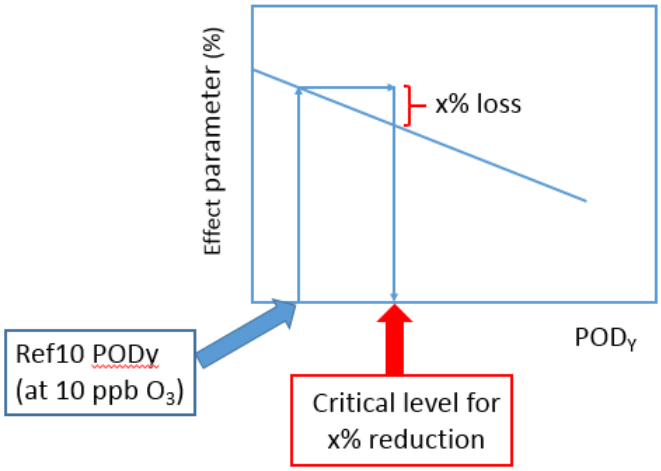

Figure III.1: *Method for using Ref10 POD$_Y$ (i.e. POD$_Y$ at 10 ppb constant O_3) as reference point for O_3 critical level derivation.*

III.3.2 WHICH METRIC TO CHOOSE AND INPUT DATA REQUIRED?

The flow chart below (Figure III.2) and table of input requirements (Table III.5) are provided to help users to choose which metric to use, depending on data availability and application.

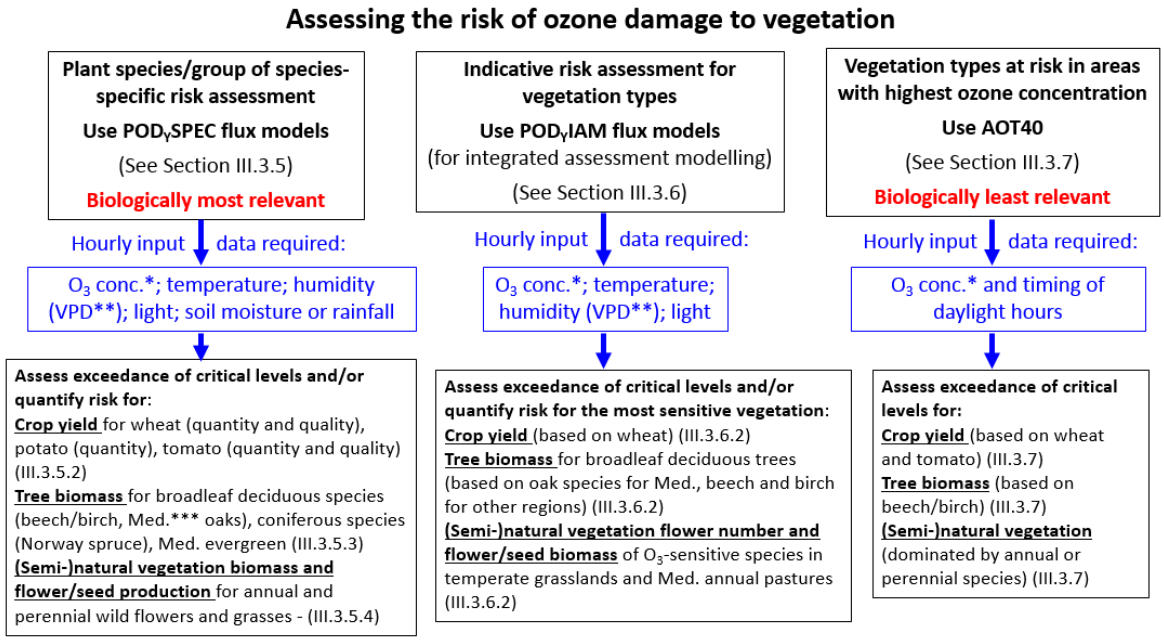

Figure III.2: *Flow chart describing which metric and critical level should be used to assess the risk of O_3 damage to vegetation, depending on availability of hourly input data and application. Additional information required for POD$_Y$SPEC and POD$_Y$IAM include biogeographical region, land cover, average canopy height and average leaf dimension and for POD$_Y$SPEC also detailed info on plant phenology. * At canopy height; ** VPD = vapour pressure deficit; *** Med. = Mediterranean.*

The biologically most relevant risk assessment will be achieved by calculating POD$_Y$SPEC, using biogeographical region-specific O_3 flux models and critical levels for individual plant species or groups (Section III.3.5). An indicative risk assessment is achieved when using

POD_YIAM, using O_3 flux models and critical levels developed for use in large-scale modelling, including integrated risk assessment (IAM; Section III.3.6). The least biologically relevant risk assessment involves calculating the O_3 concentration-based metric AOT40 (Section III.3.7). However, as mentioned before, AOT40 can be used in cases where only O_3 concentration data are available and/or areas where no climatic or water restrictions to stomatal O_3 flux are expected.

Table III.5: *Overview of hourly mean input variables required to calculate the Phytotoxic O_3 Dose above a threshold of Y (POD_YSPEC and POD_YIAM; with reference to tables - T) and to calculate AOT40.*

	Data types*	**POD_YSPEC**	**POD_YIAM**	**AOT40**
Tables to refer to for further information		Crops (T III.9), Trees (T III.11), (Semi-)natural vegetation (T III.13)	Crops, Trees, (Semi-)natural vegetation (All T III.15)	Crops, Trees, (Semi-)natural vegetation
O_3 concentration at the top of the canopy (ppb)	Measured or scaled to canopy height from measurements	√	√	√
Temperature (°C)	Measured	√	√	
Vapour pressure deficit (humidity parameter, kPa)	Calculated from measured relative humidity, temperature and atmospheric pressure	√	√	
Light (PPFD, µmol m^{-2} s^{-1})	Measured or estimated from time and geographical position	√	√	√ (astronomic daytime can also be used).
Soil water potential (kPa) or plant available water (%)	Measured or calculated using models (e.g. within DO_3SE) from rainfall and soil characteristics	√	**	

** Additional (non-hourly) information required for POD_YSPEC and POD_YIAM include biogeographical region, land cover, average canopy height and average leaf dimension and for POD_YSPEC also detailed info on plant phenology.*

*** Some chemical transport models (e.g. EMEP) used for application in integrated assessment modelling (IAM) use a simplified metric for soil water (e.g. soil moisture index; SBD-B, Simpson et al., 2012).*

III.3.3 POD_YSPEC, POD_YIAM AND AOT40-BASED CRITICAL LEVELS FOR VEGETATION

Table III.6 lists for which effects O_3 critical levels are currently available for different types of vegetation from different biogeographic regions of Europe; currently, no critical levels are available for alpine regions. The final column of the table indicates the sections with further

Table III.6: *List of effects for which O_3 critical levels are available for vegetation.*

Species or vegetation type	Effect parameter	Biogeographical region*	Ozone metric	Section	Flux model parameters, critical levels (Table - T), response functions (Figure - F)
Species-specific critical levels, using $POD_Y SPEC$ (mmol m^{-2} PLA)					
Crops					
Wheat	Grain yield, 1000-grain weight, protein yield	A,B,C,M (S,P)**	POD_6SPEC	III.3.5.2	T III.9-10, F III.10
Potato	Tuber yield	A,B,C (M,S,P)	POD_6SPEC	III.3.5.2	T III.9-10, F III.11
Tomato	Fruit yield, fruit quality	M (A,B, C,S,P)	POD_6SPEC	III.3.5.2	T III.9-10, F III.11
Forest trees					
Beech/birch	Total biomass	B,C (A,S,P)	POD_1SPEC	III.3.5.3	T III.11-12, F III.12
Norway spruce	Total biomass	B,C (A,S,P)	POD_1SPEC	III.3.5.3	T III.11-12, F III.12
Deciduous oak species	Root biomass, total biomass	M	POD_1SPEC	III.3.5.3	T III.11-12, F III.12
Evergreen tree species	Above-ground biomass	M	POD_1SPEC	III.3.5.3	T III.11-12, F III.12
(Semi-)natural vegetation					
Temperate perennial grasslands (O_3-sensitive species)	Above-ground biomass, total biomass, flower number	A,B,C (S,P)	POD_1SPEC	III.3.5.4	T III.13-14, F III.13
Mediterranean annual pasture (O_3-sensitive species)	Above-ground biomass, flower/seed biomass	M	POD_1SPEC	III.3.5.4	T III.13-14, F III.14
Vegetation-type critical levels, using $POD_Y IAM$ (mmol m^{-2} PLA)					
Crops	Grain yield	A,B,C, M (S,P)**	POD_3IAM	III.3.6.2	T III.15-16, F III.15
Forest trees					
Broadleaf deciduous	Total biomass	B,C (A,S,P)	POD_1IAM	III.3.6.2	T III.15-16, F III.15
		M	POD_1IAM	III.3.6.2	T III.15-16, F III.15
(Semi-)natural vegetation					
Temperate perennial grasslands	Flower number	A,B,C (S,P)	POD_1IAM	III.3.6.2	T III.15-16, F III.15
Mediterranean annual pasture	Seed/flower biomass	M	POD_1IAM	III.3.6.2	T III.15-16, F III.15
Concentration-based critical levels, using AOT40 (ppm h)					
Agricultural crops	Yield	All	AOT40	III.3.7.3	T III.17
Horticultural crops	Yield	All	AOT40	III.3.7.3	T III.17
Forest trees	Total biomass	All	AOT40	III.3.7.3	T III.17
(Semi-)natural vegetation dominated by annuals	Above-ground biomass	All	AOT40	III.3.7.3	T III.17
(Semi-)natural vegetation dominated by perennials	Above-ground biomass	All	AOT40	III.3.7.3	T III.17

** A= Atlantic, B = Boreal, C = Continental, M = Mediterranean, P = Pannonian, S = Steppic; critical levels are also considered applicable to regions shown in brackets, based on expert judgement.*

*** Different parameterisations for Mediterranean and non-Mediterranean species or varieties.*

details, the table of the relevant flux-model parameterisation and the figure that contains the response function from which the critical level was derived.

III.3.4 METHOD FOR MODELLING STOMATAL O_3 FLUX AND CALCULATING CRITICAL LEVEL EXCEEDANCE

O_3 stomatal flux is calculated at the leaf level at the top of the canopy using the DO_3SE (Deposition of O_3 for Stomatal Exchange) model (Büker et al., 2015; Emberson et al., 2000a,b, 2001, 2007). The DO_3SE model is available in downloadable form at http://sei-international.org/do3se.

Several steps (1-6) are required to model the stomatal flux of O_3 at leaf level at the top of the canopy and calculate critical level exceedance, and to calculate the percentage of effect (step 7) based on the slope of the flux-effect relationships, as listed in Box 4 and described in detail in Sections III.3.4.1 to III.3.4.7.

Box 4: Steps to be taken to calculate exceedance of flux-based (POD_YSPEC or POD_YIAM) critical levels and quantification of the risk of effect

1. Decide on the species and biogeographical region(s) to be included;
2. Obtain the O_3 concentrations at the top of the canopy for the species or vegetation-specific accumulation period;
3. Calculate the hourly stomatal conductance of O_3 (g_{sto});
4. Model the hourly stomatal flux of O_3 (F_{st});
5. Calculation of POD_Y (POD_YSPEC or POD_YIAM) from F_{st};
6. Calculation of exceedance of flux-based critical levels;
7. Quantification the extent of risk and calculating percentage effect due to O_3.

III.3.4.1 STEP 1: DECIDE ON THE SPECIES AND BIOGEOGRAPHICAL REGION(S) TO BE INCLUDED

Plant stomatal functioning varies per plant species and can vary by biogeographical region, reflecting different adaptations of plants to climate and soil water in these regions. To accommodate these differences, separate parameterisations and accumulation periods have been developed for stomatal O_3 flux models for different species and biogeographical regions. The EEA (2016) classification of biogeographical zones is recommended for application to risk assessments for Europe (Figure III.3); similar classifications should be applied outside of this region. For derivation of the critical levels, no data were available from Steppic and Pannonian regions, hence the applicability of critical levels for these regions is less certain. Currently, no critical levels are available for Alpine regions.

Note: In earlier versions of this Chapter, countries were assigned to a climate zone (Northern Europe, Atlantic Central Europe, Continental Central Europe, Eastern and Western Mediterranean). This classification has now been replaced by the use of biogeographical zones.

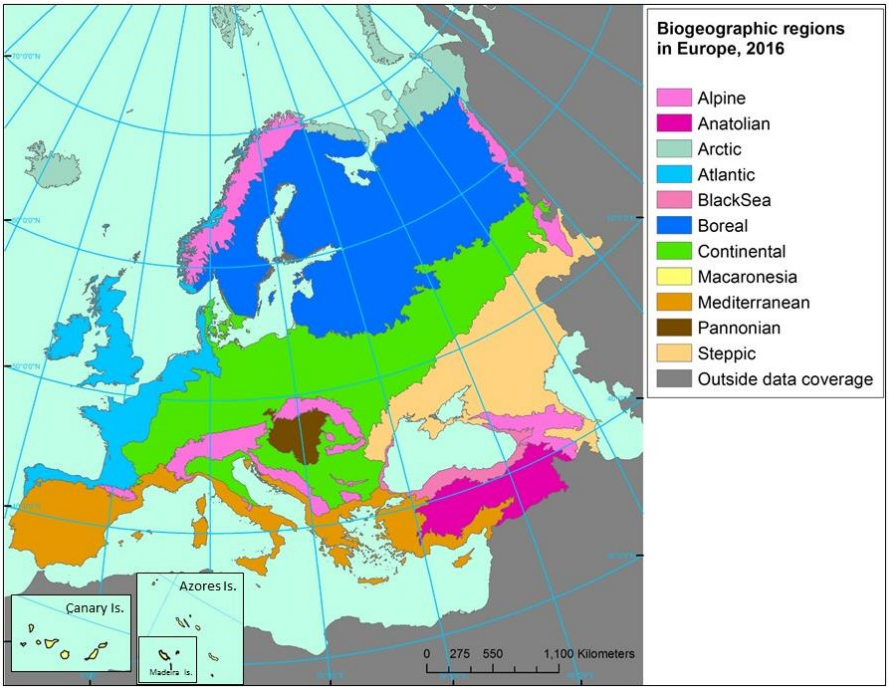

Figure III.3: *Biographic regions in Europe (EEA, 2016: http://www.eea.europa.eu/data-and-maps/data/biogeographical-regions-europe-3)*

III.3.4.2 STEP 2. OBTAIN THE O_3 CONCENTRATION AT THE TOP OF THE CANOPY FOR THE SPECIES OR VEGETATION-SPECIFIC ACCUMULATION PERIOD

Calculation of stomatal flux (or AOT40, see Section III.3.7.2) is based on hourly mean O_3 concentrations in units of parts per billion (ppb volume/volume). Where O_3 concentrations require conversion from µg m^{-3} to ppb, a conversion factor appropriate for standard temperature and pressure conditions (293.15 K, 101325 Pa) of 2 µg m^{-3} per ppb can be applied. Alternatively, the equations described in detail in Gerosa et al. (2012) could be used if temperature and atmospheric pressure are available.

In this step, the O_3 concentration at the top of the leaf canopy of the vegetation of interest is determined. This is needed because surface O_3 concentrations generally increase with increasing height above-ground. Thus, O_3 data from monitoring stations where the inlet is placed at heights of e.g. 2 – 5 m above the ground will overestimate the O_3 concentration at the canopy height of crops or low (semi-)natural vegetation such as grasslands, and will underestimate the O_3 concentration at the top of the canopy of forests.

Conversion of O_3 concentrations at measurement height to canopy height can be best achieved with an appropriate deposition model (see SBD-A). However, if suitable meteorological data are unavailable, a simple tabulation of O_3 gradients can be used (Table III.7). This table provides the average relationship between O_3 concentrations at selected heights, derived from runs of the EMEP model over May-July, selecting noon as representative of daytime (Simpson et al., 2012). O_3 concentrations are normalised by setting the 20 m value to 1.0. For example, with 30 ppb measured at 3 m height (above ground level) in a crop field, the concentration at 1 m would be 30.0 * (0.88/0.95) = 27.8 ppb. If measured in short grasslands at 3 m height, one would obtain 30.0 * (0.74/0.96) = 23.1 ppb at a canopy height of 0.1 m and for forests one would obtain 30.0 * (1/0.96) = 31.3 ppb at a canopy height of 20 m.

Table III.7: *Representative O_3 gradients above artificial (1 m) crop, and short grasslands (0.1 m). O_3 concentrations are normalised by setting the 20 m value to 1.0. These gradients are derived from noontime factors and are intended for daytime use only.*

Measurement height above the ground [m]	**O_3 concentration gradient**	
	Crops (where z_1=1m, g_{max}= 450 mmol O_3 m^{-2} PLA s^{-1})	**Short Grasslands and Forest Trees** (where z_1=0.1m, g_{max}=270 mmol O_3 m^{-2} PLA s^{-1})
20	1.0	1.0
10	0.99	0.99
5	0.97	0.97
4	0.96	0.97
3	0.95	0.96
2	0.93	0.95
1	0.88	0.92
0.5	0.81*	0.89
0.2	-	0.83
0.1	-	0.74

** 0.5m is below the displacement height of crops, but may be used for taller grasslands, see text.*

III.3.4.3 STEP 3. CALCULATE THE HOURLY STOMATAL CONDUCTANCE OF O_3 (g_{sto})

The core of the leaf O_3 flux model is the stomatal conductance (g_{sto}) multiplicative algorithm included in the DO_3SE model and incorporated within the EMEP O_3 deposition module (Simpson et al., 2012), proposed by Jarvis (2016) and modified by Emberson et al. (2000a,b). The multiplicative algorithm has the following formulation:

(III.1) $$g_{sto} = g_{max} * [\min(f_{phen}, f_{O3})] * f_{light} * \max\{f_{min}, (f_{temp} * f_{VPD} * f_{SW})\}$$

Where g_{sto} is the actual stomatal conductance (mmol O_3 m^{-2} PLA s^{-1}) and g_{max} is the species-specific maximum stomatal conductance (mmol O_3 m^{-2} PLA s^{-1}).

The parameters f_{phen}, f_{O3}, f_{light}, f_{temp}, f_{VPD}, f_{SW} and f_{min} are all expressed in relative terms (i.e. they take values between 0 and 1 as a proportion of g_{max}). These parameters allow for the modifying influence on stomatal conductance to be estimated for growth stage such as flowering or release of dormancy, or phenology (f_{phen}), O_3 concentration (f_{O3}, only used for crops), and four environmental variables: light (irradiance, f_{light}), temperature (f_{temp}), atmospheric water vapour pressure deficit (VPD, a measure of air humidity, f_{VPD}) and soil water (SW; soil water potential, f_{SW}, measure of soil moisture, replaced by f_{PAW} for crops where PAW is the plant available water content); f_{min} is the relative minimum stomatal conductance that occurs during daylight hours.

Each parameter modifies the maximum stomatal conductance in different ways. For example, stomatal conductance gradually increases as temperature increases reaching an optimum and then gradually declines as temperature increases beyond the optimum, whilst stomatal conductance increases rapidly as light levels increase, reaching a maximum at relatively low light levels and is maintained at that maximum as light levels increase further. Illustrations of the modifying effect of each factor on stomatal conductance are provided (Figures III.4-9). Hourly values of all driving variables are required to calculate g_{sto} using Equation III.1, and in step 4 (see Box 4), the stomatal O_3 flux (F_{st}), with hourly time resolution. In step 5, the hourly values of F_{st} are summed to obtain the total Phytotoxic O_3

Dose above a flux-threshold Y (POD_Y). Table III.8 lists all the input variables and parameters required to calculate POD_YSPEC and POD_YIAM and the sources of this information.

Table III.8: *Parameters included in the DO_3SE model for calculating POD_YSPEC and POD_YIAM; f_{phen} and f_{SW} are not included in POD_YIAM.*

Parameter	Source	POD_YSPEC	POD_YIAM
g_{max}	Parameterisation table	√	√
f_{min}	Parameterisation table	√	√
f_{phen}	Calculated using formulae and fixed parameters in table	√	
f_{light}	Calculated using formulae and fixed parameters in table	√	√
f_{temp}	Calculated using formulae and fixed parameters in table	√	√
f_{VPD}	Calculated using formulae and fixed parameters in table	√	√
f_{SW} (or f_{PAW})	Calculated using formulae and fixed parameters in table	√ f_{PAW} can be used for crops as an alternative	*

** Included in the EMEP Model as soil moisture index (Simpson et al., 2012).*

III.3.4.3.1 *G_{MAX} AND F_{MIN}*

Species- or vegetation type-specific values are provided in the relevant parameterisation tables for g_{max} and f_{min} based on analysis of published data (see SBD-A for further details); g_{max} values provided here are in mmol O_3 m^{-2} PLA s^{-1}. These have been converted from g_{max} (water vapour) using a conversion factor of 0.663 to account for the difference in the molecular diffusivity of water vapour in relation to that of O_3 (Massman,1998; Grünhage et al., 2012); f_{min} is the minimum daylight stomatal conductance expressed as a fraction of g_{max}.

III.3.4.3.2 *F_{PHEN}*

The phenology function is based on two approaches depending on vegetation type:

(a) For forest trees and (semi-)natural vegetation, f_{phen} is calculated according to Equations III.2a,b,c when using parameterisations based on a fixed number of days (FD; Figure III.4a);
(b) For crops, f_{phen} is calculated according to Equations III.3a,b,c, using parameterisations based on effective temperature sum accumulation (ETS).

Each pair of equations gives f_{phen} in relation to the yearly accumulation period for POD_YSPEC where A_{start} and A_{end} are the start and end of the accumulation period respectively. The subscripts FD (e.g. A_{start_FD}) and ETS (e.g. A_{start_ETS}) refer to the fixed day and effective temperature sum method, respectively.

a)

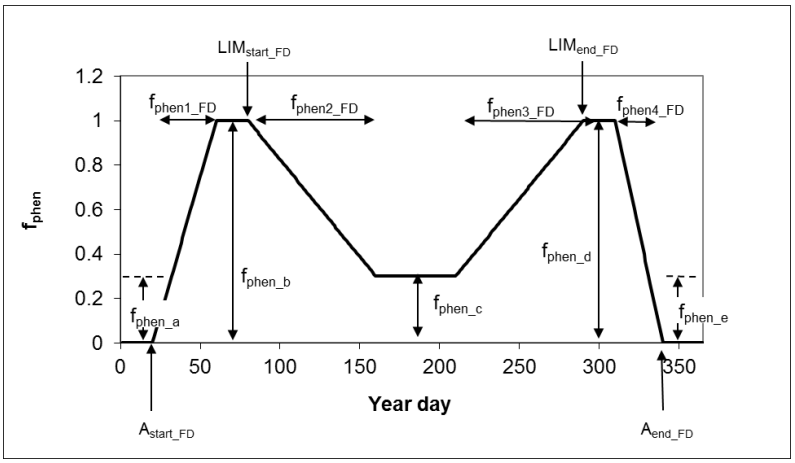

b)

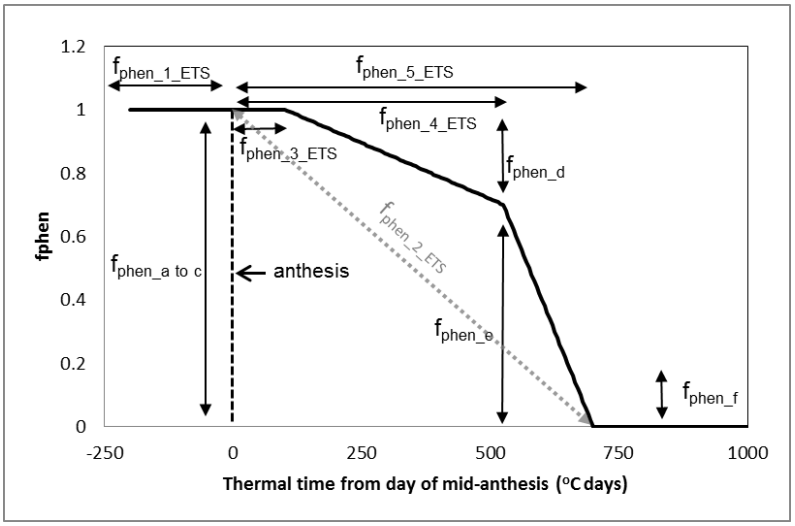

Figure III.4: *An illustration of the formulation of f_{phen} using a) a fixed number of days, as used for forest trees and (semi-)natural vegetation (example shown here for Mediterranean trees with summer dip in f_{phen} to simulate the effect of mid-season water photo-oxidative stress on stomatal conductance, see Equation III.23), and b) effective temperature sum accumulation, as used for crops. Note: example shown here is for wheat, with effective temperature sum accumulated from day of mid-anthesis in three steps ($f_{phen\_3\_ETS}$, $f_{phen\_4\_ETS}$ and $f_{phen\_5\_ETS}$); $f_{phen\_2\_ETS}$ can replace these three steps and is usually not used for wheat, but is used for potato and tomato (hence shown in grey colour here). For potato and tomato the effective temperature sum is accumulated from day of tuber initiation and from the day of planting at the 4th true leaf stage respectively.*

The phenology function consists of terms describing rate changes of g_{max} ($f_{phen\_a\text{-}e}$; expressed as fractions) and time periods describing the duration from one phenology stage to another ($f_{phen\_1\text{-}5}$; expressed as days (method (a)) or growing degrees days (method (b)).

The parameters f_{phen_a} and f_{phen_e} denote the maximum fraction of g_{max} at A_{start} and A_{end}. $f_{phen\_b\text{-}d}$ and $f_{phen\_1\text{-}5}$ are species- or vegetation type-specific parameters describing the shape of the function within the accumulation period.

Method (a): based on a fixed time interval

when $A_{start\_FD} \leq yd < (A_{start\_FD} + f_{phen\_1\_FD})$

(III.2a) $f_{phen} = (1 - f_{phen\_a}) * ((yd - A_{start\_FD})/f_{phen\_1\_FD}) + f_{phen\_a}$

when $(A_{start} + f_{phen\_1\_FD}) \leq yd \leq (A_{end} - f_{phen\_4\_FD})$

(III.2b) $f_{phen} = 1$

when $(A_{end} - f_{phen\_4\_FD}) < yd \leq A_{end}$

(III.2c) $f_{phen} = (1 - f_{phen\_e}) * ((A_{end} - yd)/f_{phen\_4\_FD}) + f_{phen\_e}$

where yd is the year day; A_{start} and A_{end} are the year days for the start and end of the O_3 accumulation period respectively.

Method (b): based on temperature sum accumulation

when $A_{start\_ETS} \leq ETS < (A_{start\_ETS} + f_{phen\_1\_ETS})$

(III.3a) $$f_{phen} = 1 - \left(\frac{1 - f_{phen\_a}}{f_{phen\_1\_ETS}} \right) \left((A_{start\_ETS} + f_{phen\_1\_ETS}) - ETS \right)$$

when $(A_{start\_ETS} + f_{phen\_1\_ETS}) \leq ETS \leq (A_{end\_ETS} - f_{phen\_2\_ETS})$

(III.3b) $f_{phen} = 1$

when $(A_{end\_ETS} - f_{phen\_2\_ETS}) < ETS \leq A_{end\_ETS}$

(III.3c) $$f_{phen} = 1 - \left(\frac{1 - f_{phen\_e}}{f_{phen\_2\_ETS}} \right) \left(ETS - (A_{end\_ETS} - f_{phen\_2\_ETS}) \right)$$

where ETS is the effective temperature sum in ˚C days using a base temperature of 0 ˚C and A_{start_ETS} and A_{end_ETS} are the effective temperature sums (above a base temperature of 0 ˚C) at the start and end of the O_3 accumulation period respectively. As such, A_{start_ETS} will be equal to 0 ˚C days. Note: A base temperature of 0 °C is currently recommended for wheat and potato.

III.3.4.3.3 F_{LIGHT}

Leaf stomata respond to light as indicated in Figure III.5. This stomatal response is used to define f_{light} (Equation III.4). Species (for POD_YSPEC) or vegetation type specific (for POD_YIAM) values for $light_a$ are provided in the parameterisation tables.

(III.4) $f_{light} = 1 - EXP((-light_a)*PPFD)$

where PPFD represents the photosynthetic photon flux density in units of μmol m^{-2} s^{-1}.

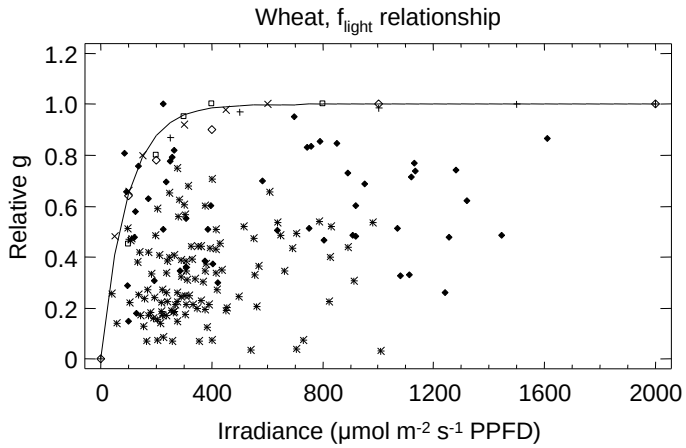

Figure III.5: *Illustration of the f_{light} function, using wheat as an example (Pleijel et al., 2007).*

III.3.4.3.4 *F_{TEMP}*

Leaf stomata respond to temperature (T, air temperature in ˚C) as indicated in Figure III.6. This stomatal response is used to define f_{temp} (Equations III.5a,b). Species (for POD_YSPEC) or vegetation type specific (for POD_YIAM) values for T_{min} and T_{max} (the minimum and maximum temperatures at which stomatal closure occurs, respectively) and the optimum temperature (T_{opt}) are provided in the parameterisation tables.

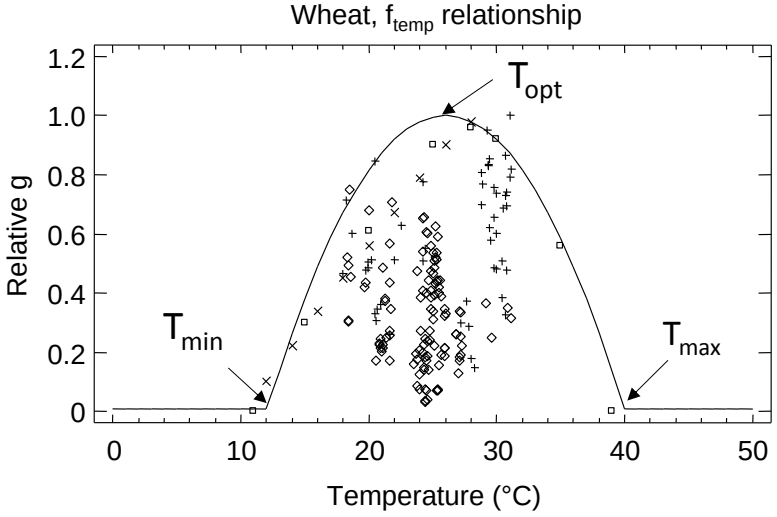

Figure III.6: *Illustration of the f_{temp} function, using wheat as an example (Pleijel et al., 2007).*

The function used to describe f_{temp} is given in Equations III.5a,b:

when $T_{min} < T < T_{max}$

(III.5a) $f_{temp} = \max \{f_{min}, [(T - T_{min}) / (T_{opt} - T_{min})] * [(T_{max} - T) / (T_{max} - T_{opt})]^{bt}\}$

when $T_{min} > T > T_{max}$

(III.5b) $f_{temp} = f_{min}$

and bt is calculated as:

(III.6) $bt = (T_{max} - T_{opt}) / (T_{opt} - T_{min})$

III.3.4.3.5 *F_{VPD} AND ΣVPD ROUTINE*

The leaf stomatal response to air humidity is defined using vapour pressure deficit (VPD in kPa), which is the drying power of the air. VPD can be calculated from air temperature and air relative humidity. VPD (Equation III.7) is defined as the difference between the potential water vapour pressure, $e_s(T_a)$, at the prevailing air temperature T_a, and the actual water vapour pressure of the air e_a:

(III.7) $$\mathrm{VPD} = \mathrm{e_s}(\mathrm{T_a}) - \mathrm{e_a} = \mathrm{e_s}(\mathrm{T_a})(1 - \mathrm{h_r})$$

and can be calculated from T_a (given in °C) and relative humidity (h_r, the most often reported variable describing air humidity; Equations III8a,b)

(III.8a) $$\mathrm{h_r} = \frac{\mathrm{e_a}}{\mathrm{e_s}(\mathrm{T_a})}$$

once $e_s(T_a)$ has been obtained from the formula

(III.8b) $$\mathrm{e_s}(\mathrm{T_a}) = \mathrm{a}\exp\left(\frac{\mathrm{bT_a}}{\mathrm{T_a}+\mathrm{c}}\right)$$

where a, b and c are empirical constants (a = 0.611 kPa, b = 17.502, c = 240.97°C). Further details can be obtained from Campbell & Norman (2000).

The response of leaf stomata to the VPD of the air surrounding the leaves is included in two ways:

(i) f_{VPD}

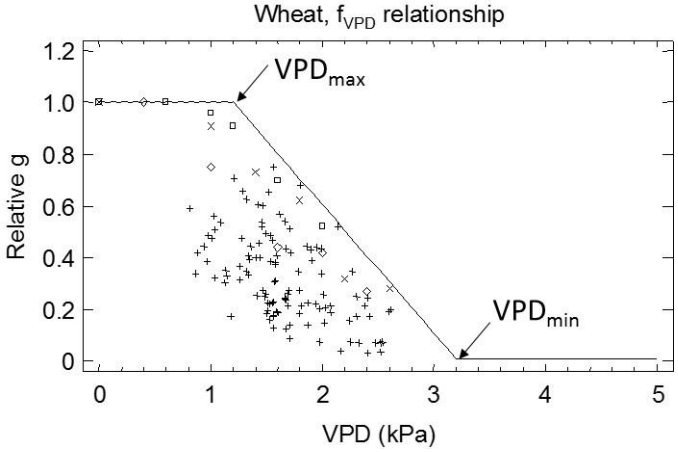

Figure III.7: *Illustration of the f_{VPD} function, using wheat in non-Mediterranean areas as an example (Pleijel et al., 2007).*

Applicable to all species and vegetation types, this function describes the response shown in Figure III.7. As VPD increases (i.e. the air becomes more dry) above a threshold value of VPD (VPD_{max}; VPD where g_{sto} is at maximum), the stomatal pores begin to close until a maximum VPD value is reached at which the stomatal pores are fully closed (VPD_{min}) and conductance (g_{sto}) is at a minimum value. This response of the stomata to VPD is described by the f_{VPD} function (Equation III.9):

(III.9) $f_{VPD} = \min\{1, \max\{f_{min}, ((1-f_{min})*(VPD_{min} - VPD) / (VPD_{min} - VPD_{max})) + f_{min}\}\}$

(ii) ΣVPD

For POD_YSPEC for crops, an additional effect of VPD is included. During the afternoon the temperature typically decreases, which is normally followed by a decline in VPD. The f_{VPD} function would then suggest stomatal re-opening, but this does not usually happen in crops. During the day plants lose water through transpiration faster than water is replaced by root uptake, resulting in a reduction of the plant water potential, preventing stomatal re-opening. The plant water potential recovers during the night when transpiration is low. To model this effect, the hourly VPD values during the daylight hours (when global radiation is more than 50 W m^{-2}) are summed as ΣVPD (Uddling et al., 2004). A large ΣVPD is related to large transpiration. If the ΣVPD exceeds a certain value, stomatal re-opening in the afternoon is prevented in the model:

If $\Sigma VPD \geq \Sigma VPD\_crit$, then:

$g_{sto\_hour\_n+1} \leq g_{sto\_hour\_n}$

Where $g_{sto\_hour\_n}$ and $g_{sto\_hour\_n+1}$ are the g_{sto} values for hour n and hour n+1 respectively calculated according to Equation III.1

ΣVPD (kPa) should be calculated for daylight hours until dawn of the next day. If $\Sigma VPD \geq \Sigma VPD_{crit}$, g_{sto} calculated using Equation III.1 is valid if smaller or equal to g_{sto} of the preceding hour. If g_{sto} is larger than g_{sto} of the preceding hour, given that ΣVPD is larger than or equal to ΣVPD_{crit}, it is replaced by the g_{sto} of the preceding hour.

III.3.4.3.6 *F_{SW}*

For POD_YIAM, f_{SW} is set to have no effect within the calculation of g_{sto}. However, the effect of soil moisture is important and in large-scale applications, surrogate indices are usually applied such as the Soil Moisture Index in the EMEP model (Simpson et al., 2012).

For POD_YSPEC, f_{SW} uses soil water potential (SWP) to determine the leaf stomatal response to soil drying. The function takes the shape indicated in Figure III.8 and is given in Equation III.10):

(III.10) $f_{SW} = \min\{1, \{f_{min}, ((1-f_{min})*(SWP_{min}-SWP) / (SWP_{min} - SWP_{max})) + f_{min}\}\}$

Where SWP_{min} is the minimum SWP for stomatal conductance and SWP_{max} is the SWP above which conductance is maximum.

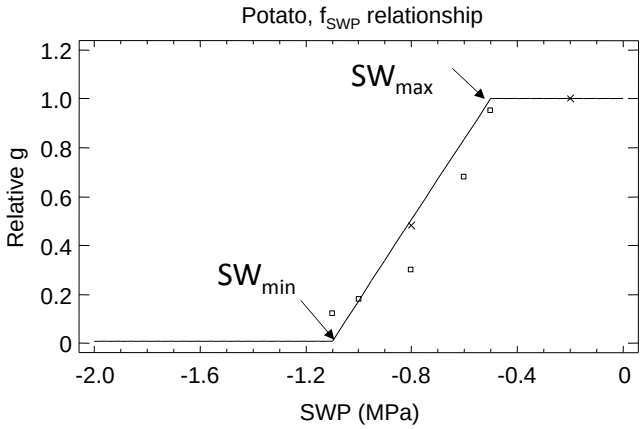

Figure III.8: *Illustration of the f_{SW} function, using soil water potential (SWP) for potato as an example*

Note: For crop species such as wheat, root zone Plant Available Water (PAW) can be used instead of SWP in f_{SW}. PAW is the amount of water in the soil (%) which is available to the plants. At PAW = 100% the soil is at field capacity, at PAW = 0% the soil is at wilting point. PAW_t is the threshold PAW, above which stomatal conductance is at a maximum, i.e. the function used to describe f_{PAW} is given in Equation III.11 and the shape of the response is indicated in Figure III.9:

when $PAW_t \leq PAW \leq 100$ %,

$f_{PAW} = 1$

whilst, when $PAW < PAW_t$

(III.11) $$f_{\mathrm{PAW}} = 1 + \frac{PAW - PAW_{\mathrm{t}}}{PAW_{\mathrm{t}}}$$

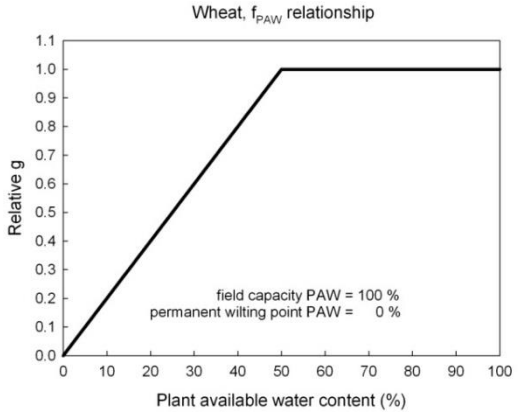

Figure III.9: *Illustration of the f_{PAW}, using wheat as an example f_{PAW} for wheat (Grünhage et al., 2012).*

III.3.4.3.7 F_{O3}

For wheat and potato in POD_6SPEC only, a function is included to allow for the influence of O_3 on stomatal flux by promoting premature senescence, as described for wheat by Danielsson et al. (2003) and for potato by Pleijel et al. (2002). As such this function is used in association with the f_{phen} function to estimate g_{sto}. The f_{O3} function typically operates over a one-month period and only comes into operation if it has a stronger senescence-promoting effect in reducing stomatal conductance than normal senescence. Equations are provided for wheat and potato in Section III.3.5.2.1.

III.3.4.4 STEP 4. MODELLING HOURLY STOMATAL FLUX OF O_3 (F_{ST})

The stomatal flux of O_3 (F_{st}) is calculated based on the assumption that the concentration of O_3 at the top of the canopy represents a reasonable estimate of the concentration at the upper surface of the laminar layer for a sunlit upper canopy leaf (e.g. flag leaf for wheat). If $c(z_1)$ is the concentration of O_3 at canopy top (height z_1, unit: m), in nmol m^{-3}, then F_{st} (nmol m^{-2} PLA s^{-1}), is given by Equation 12a. Equation 15 shows how to convert the O_3 concentration from ppb to nmol m^{-3}. In order to be used correctly in Equations III.12a and III.12b, g_{sto} from equation III.1 has to be converted from units mmol m^{-2} s^{-1} to units m s^{-1}. At standard temperature (20 ^{o}C) and air pressure (1.013×10^5 Pa), the conversion is made by dividing the conductance value expressed in mmol m^{-2} s^{-1} by 41000 to give conductance in m s^{-1}.

(III.12a) $$F_{st} = c(z_1) * \frac{1}{r_b + r_c} * \frac{g_{sto}}{g_{sto} + g_{ext}}$$

The $1/(r_b+r_c)$ term represents the deposition rate to the leaf through resistances r_b (quasi-laminar resistance) and r_c (leaf surface resistance). The fraction of this O_3 taken up by the stomata is given by $g_{sto}/(g_{sto}+g_{ext})$, where g_{sto} is the stomatal conductance, and g_{ext} is the external leaf, or cuticular, resistance. As the leaf surface resistance, r_c, is given by $r_c = 1/(g_{sto} + g_{ext})$, we can also write Equation III.12a as:

(III.12b) $$F_{st} = c(z_1) * g_{sto} * \frac{r_c}{r_b + r_c}$$

A value for g_{ext} has been chosen to keep consistency with the EMEP deposition modules "big-leaf" external resistance, $R_{ext} = 2500/SAI$, where SAI is the surface area index (green + senescent LAI). Assuming that SAI can be simply scaled:

(III.13) $$g_{ext} = 1/2500 \quad [\text{m s}^{-1}]$$

Consistency of the quasi-laminar boundary layer is harder to achieve, so the use of a leaf-level r_b term (McNaughton & van den Hurk, 1995) is suggested, making use of the cross-wind leaf dimension L (i.e. leaf width; unit: m) and the wind speed at height z_1, $u(z_1)$:

(III.14) $$r_b = 1.3 * 150 * \sqrt{\frac{L}{u(z_1)}} \quad [\text{s m}^{-1}]$$

Where the factor 1.3 accounts for the differences in diffusivity between heat and O_3.

To convert the O_3 concentration (C) at canopy height from ppb to nmol m^{-3}, the following equation should be used:

(III.15) C [nmol m^{-3}] = C [ppb] * P/(RT)

Where P is the atmospheric pressure in Pa, R is the universal gas constant of 8.31447 J mol^{-1} K^{-1} and T is the air temperature in degrees Kelvin. At standard temperature (20 ^oC) and air pressure (1.013×10^5 Pa), the concentration in ppb should be multiplied by 41.56 to calculate the concentration in nmol m^{-3}.

III.3.4.5 STEP 5. CALCULATION OF POD_Y (POD_YSPEC OR POD_YIAM)

Hourly averaged stomatal O_3 fluxes (F_{st}) in excess of a Y threshold are accumulated over a species or vegetation-specific accumulation period using the following equation:

(III.16) $$POD_Y = \sum[(F_{st}-Y)\cdot(3600/10^6)] \text{ (mmol m}^{-2}\text{ PLA)}$$

The value Y (nmol m^{-2} PLA s^{-1}) is subtracted from each hourly averaged F_{st} (nmol m^{-2} PLA s^{-1}) value only when $F_{st}>Y$, during daylight hours (when global radiation is more than 50 W m^{-2}). The value is then converted to hourly fluxes by multiplying by 3600 and to mmol by dividing by 10^6 to get the stomatal O_3 flux in mmol m^{-2} PLA.

Species- or vegetation-specific flux threshold values of Y and accumulation periods are provided in the relevant sections.

III.3.4.6 STEP 6. CALCULATION OF EXCEEDANCE OF FLUX-BASED CRITICAL LEVELS

If the calculated POD_Y value is larger than the flux-based critical level for O_3, then there is exceedance of the critical level ($CL_{exceedance}$). Exceedance of the critical level is calculated at follows:

(III.17) $CL_{exceedance} = POD_Y$ – critical level

III.3.4.7 STEP 7. QUANTIFICATION OF EXTENT OF RISK AND CALCULATING PERCENTAGE EFFECT DUE TO O_3

Quantification of the level of risk is based on the slope of flux-effect relationships, without taking the intercept of the response function into account.

For each POD_YSPEC critical level, the percentage effect is provided per mmol m^{-2} PLA, for quantifying the potential maximum magnitude of effect. Hence, the percentage effect due to O_3 impact should be calculated as follows:

(III.18a) (POD_YSPEC – Ref10 POD_YSPEC) * % reduction per mmol m^{-2} POD_YSPEC

For POD_YIAM, the above approach can only be applied for crops, not for forest trees or (semi-)natural vegetation. Hence, the percentage effect due to O_3 impact on crop yield estimated in large-scale modelling should be calculated as follows:

(III.18b) (POD_YIAM – Ref10 POD_YIAM) * % reduction per mmol m^{-2} POD_YIAM.

III.3.5 SPECIES-SPECIFIC FLUX EFFECT RELATIONSHIPS AND CRITICAL LEVELS FOR DETAILED ASSESSMENTS OF RISK (USING POD_YSPEC)

III.3.5.1 APPLICATION

POD_YSPEC O_3 flux models have been derived for a number of crop, forest trees and (semi-)natural vegetation species using the modelling approach described in Section III.3.4. These species-specific flux models have been used to derive flux-effect relationships and critical levels based on POD_YSPEC. Their application is described in Box 5. Additional flux models are included in SBD-A for receptors for which a robust flux model is available but a flux-effect relationship is not currently available, and are suitable for mapping risk of effects without quantification of the extent of damage.

Box 5: Applications for species-specific flux-effect relationships and critical levels

The species-specific flux models and associated response functions and critical levels are the most biologically relevant. They can be used at any geographical scale and are particularly useful for application at the local scale to quantify the degree of risk to a specific species or a group of plant species. For several species, biogeographical region-specific flux parameterisations are included.

III.3.5.2 CROPS

III.3.5.2.1 *PARAMETERISATION OF THE O_3 STOMATAL FLUX MODEL FOR CROPS*

The parameterisations recommended for use in calculating POD_6SPEC for wheat *(*bread wheat - *Triticum aestivum* and durum wheat - *Triticum durum;* Grünhage et al., 2012; González-Fernández et al., 2013), potato (*Solanum tuberosum*; Pleijel et al., 2007) and tomato (*Solanum lycopersicum*; González-Fernández et al., 2014) are shown in Table III.9. Species-specific notes to aid calculation of stomatal O_3 fluxes are found below the table.

For crops, the following additional information is required for calculating stomatal flux using the method provided in Section III.3.4.3 and the parameterisation provided in Table III.9:

Wheat

Timing of accumulation period

The accumulation period for wheat is 200 °C days before mid-anthesis (mid-point in flowering) to 700 °C days after mid-anthesis. The timing of mid-anthesis can be estimated using several methods, depending on application and availability of data, including:

- Observational data describing actual growth stages;
- Local agricultural statistics/information describing the timings of growth stages by region or country;
- Phenological growth models in conjunction with daily meteorological data;
- Fixed time periods (which may be moderated by climatic region or latitude) or growth stage intervals.

For European maps of risk, it is recommended that the timing of mid-anthesis is estimated by starting at the first date after 1 January when the temperature exceeds 0°C, or 1 January if the temperature exceeds 0°C on that date. The mean daily temperature should then be accumulated (temperature sum), and mid-anthesis is estimated to be a temperature sum of 1075 °C days, with local variation including 1256ºC days for bread wheat and 1192 ºC days for durum wheat in Spain (González-Fernández et al., 2013) and 1089 – 1102 days for winter wheat cultivars in France (Grünhage et al., 2012). Where suitable temperature data is not available, the timing of mid-anthesis for both spring and winter wheat can be approximated as a function of latitude (degrees N) using Equation III.19:

(III.19) Mid-anthesis = 2.57 * latitude + 40

Table III.9: *Parameterisation of the DO_3SE model for POD_6SPEC for wheat flag leaves and the upper-canopy sunlit leaves of potato and tomato.*

Parameter	Units	Crop species parameterisation – POD_6SPEC				
Region *(may also be applicable in these regions)*		Atlantic, Boreal, Continental (*Pannonian, Steppic)*	Mediterranean	Mediterranean	Atlantic, Boreal, Continental (*Mediterranean, Pannonian, Steppic)*	Mediterranean
Species	Common name	**(Bread) Wheat**	**(Bread) Wheat**	**(Durum) Wheat**	**Potato**	**Tomato**
	Latin name	*Triticum aestivum*	*Triticum aestivum*	*Triticum durum*	*Solanum tuberosum*	*Solanum lycopersicum*

g_{max}	mmol O_3 m^{-2} PLA s^{-1}	500	430	410	750	330
f_{min}	fraction	0.01	0.01	0.01	0.01	0.06
light_a	-	0.0105	0.0105	0.0105	0.005	0.0125
T_{min}	°C	12	12	11	13	18
T_{opt}	°C	26	28	28	28	28
T_{max}	°C	40	39	45	39	37
VPD_{max}	kPa	1.2	3.2	3.1	2.1	1
VPD_{min}	kPa	3.2	4.6	4.9	3.5	4
ΣVPD_{crit}	kPa	8	16	16	10	-
PAW_t[i]	%	50	-	-	-	-
SWC_{max}[i]	% volume	-	18.6	18.0	-	-
SWC_{min}[i]	% volume	-	4.7	4.1	-	-
SWP_{max}	MPa	-	-	-	-0.5	-
SWP_{min}	MPa	-	-	-	-1.1	-
f_{O3}	POD_0 mmol O_3 m^{-2} PLA s^{-1} (wheat)	14	-	-	-	-
f_{O3}	AOT0, ppmh (potato)	-	-	-	40	-
f_{O3}	exponent	8	-	-	5	-
A_{start}_ETS	°C day	-	-	-	-	250[ii]
A_{end}_ETS	°C day	-	-	-	-	1500[ii]
Leaf dimension	cm	2	2	2	4	3 (leaflet width)
Canopy height	m	1	0.75	0.75	1	2
f_{phen_a}	fraction	0.3	0.0	0.0	0.4	1.0
f_{phen_b}	fraction	-	-	-	-	-
f_{phen_c}	fraction	-	-	-	-	-
f_{phen_d}	fraction	-	-	-	-	-
f_{phen_e}	fraction	0.7	0.99	0.99	0.2	0.0
$f_{phen\_1\_ETS}$	ºC day	-200	-300	-300	-330	0
$f_{phen\_2\_ETS}$	ºC day	0	0	0	800	2770[ii]
$f_{phen\_3\_ETS}$	ºC day	100	70	100	-	-
$f_{phen\_4\_ETS}$	ºC day	525	0	0	-	-
$f_{phen\_5\_ETS}$	ºC day	700	550	675	-	-

The values in brackets represent "dummy" values required for DO_3SE modelling purposes. "-" = parameterisation not required for this species.

[i] Soil water content (SWC) is calculated as the soil water content available for transpiration, i.e. the actual SWC minus the SWC at the wilting point. PAW_t is the threshold for plant available water (PAW), above which stomatal conductance is at a maximum.

[ii] Flux accumulation period in degree-days over a base temperature of 10 °C since the date of tomato planting in the field at the 4th true leaf stage, BBCH code of 14.

However, it should be recognised that this method is less preferable to the use of the effective temperature sum models described above since latitude is not directly related to temperature and this method will not distinguish between spring and winter wheat growth patterns.

Equation III.19 is based on data collected by the ICP Vegetation (Mills & Ball, 1998, Mills et al., 2007) from ten sites across Europe (ranging in latitude from Finland to Slovenia) describing the date of mid-anthesis of commercial winter wheat. Applying Equation III.19 across the European wheat growing region would give mid-anthesis dates ranging from the end of April to mid-August at latitudes of 35 to 65 °N respectively. These anthesis dates fall

approximately within recognised spring wheat growing seasons as described by Peterson (1965).

f_{phen}

The phenology function for wheat, based on accumulation of thermal time, should be modified as described in the equations below:

- when ($f_{phen\_2\_ETS} - f_{phen\_1\_ETS}$) ≤ ETS ≤ ($f_{phen\_2\_ETS} + f_{phen\_3\_ETS}$)

  (III.20a) $f_{phen} = 1$

- when ($f_{phen\_2\_ETS} + f_{phen\_3\_ETS}$) < ETS ≤ ($f_{phen\_2\_ETS} + f_{phen\_4\_ETS}$)

  (III.20b) $$f_{phen} = 1 - \left(\frac{f_{phen\_a}}{f_{phen\_4\_ETS} - f_{phen\_3\_ETS}} \right) (\mathrm{ETS} - f_{phen\_3\_ETS})$$

- when ($f_{phen\_2\_ETS} + f_{phen\_4\_ETS}$) < ETS ≤ $f_{phen\_5\_ETS}$

  (III.20c)

$$f_{phen} = f_{phen\_e} - (f_{phen\_e} / f_{phen\_5\_ETS} - f_{phen\_4\_ETS}) * (ETS - f_{phen\_4\_ETS})$$

where ETS is the effective temperature sum in ˚C days using a base temperature of 0˚C. As such A_{start_ETS} (itself not defined for wheat) will be at 200 ˚C days before mid-anthesis (-200 ˚C days, as defined by $f_{phen\_1\_ETS}$), mid-anthesis at 0 ˚C days and A_{end_ETS} (itself not defined for wheat) at 700 ˚C days after mid-anthesis (as defined by $f_{phen\_5\_ETS}$). The total temperature sum thus being 900 ˚C days.

f_{VPD}

Under Mediterranean conditions the stomata of wheat remain open under drier humidities (higher VPDs) than indicated with the parameterisations for f_{VPD} for non_Mediterannean climates (González-Fernández et al, 2013), and thus two climate region-specific f_{VPD} parameterisations are provided.

f_{PAW}

f_{PAW} is used instead of f_{SW} for wheat, see Equation III.11.

f_{O3}

The f_{O3} function typically operates over a one-month period and only comes into operation if it has a stronger senescence-promoting effect than normal senescence.

The O_3 function for spring wheat (based on Danielsson et al. (2003) but recalculated for projected leaf area - PLA) is:

(III.21) $f_{O3} = ((1+(POD_0/14)^8)^{-1})$, where POD_0 is accumulated from A_{start}

Potato

f_{phen}

Use the thermal time equations (Equations III.3,a,b,c). Tuber initiation has the same phenology function as anthesis has for wheat (Equations III.20a,b,c). Note that A_{start_ETS}

(itself not defined for potato) will be at 330 ˚C days before tuber initiation (-330 ˚C days, as defined by $f_{phen\_1\_ETS}$), tuber initiation at 0 ˚C days and A_{end_ETS} (itself not defined for potato) at 800 ˚C days after tuber initiation (as defined by $f_{phen\_2\_ETS}$). The total temperature sum thus being 1130 ˚C days.

f_{O3}

The O_3 function for potato (based on Pleijel et al., 2002) is:

(III.22) $f_{O3} = ((1+(AOT0/40)^5)^{-1})$, where AOT0 is accumulated from A_{start}

Tomato

g_{max}

A mean value is provided in Table III.9. Cultivar-specific values of g_{max} are provided in González-Fernández et al. (2014).

Timing of accumulation period

The accumulation period for tomato is 250ºC days to 1500ºC days after transplantation in the field over a base temperature of 10ºC (González-Fernández et al., 2014). The timing of transplantation into the field can vary widely depending on regions, years, cultivars and agronomic practices from March to July in the Northern Hemisphere (Battilani et al., 2012). Tomato transplantation date can be estimated using several methods, depending on the availability of data, including:

- Observational data describing actual growth stages;
- Local agricultural statistics/information describing the timings of growth stages by region or country;
- Phenological growth models in conjunction with daily meteorological data;
- Fixed time periods (which may be moderated by climatic region or latitude) or growth stage intervals.

For European maps of risk, it is suggested that the timing of transplantation is set on a fixed date, such as the 1st of June.

III.3.5.2.2 *FLUX-EFFECT RELATIONSHIPS AND CRITICAL LEVELS FOR CROPS*

Box 6: Applications for species-specific (POD_6SPEC) flux-effect relationships and critical levels for crops

The species-specific flux models and associated response functions and critical levels for ozone-sensitive crops and cultivars can be used to quantify the potential negative impacts of O_3 on the security of food supplies at the local and regional scale. They can be used to estimate yield losses, including economic losses.

The applications of the POD_YSPEC functions and critical levels for crops are described in Box 6. A flux-threshold Y of 6 (POD_6SPEC) provides the strongest flux-effect relationships for crops (Pleijel et al., 2007). O_3 effects proved to be significant at a 5% reduction of the

effect parameter (Mills et al., 2011b), hence critical levels were determined for a 5% reduction of the effect based on the slope of the relationship and are summarised in Table III.10, with further information on the sources of data provided in Annex 3, Table A2. The flux-effect relationships for wheat yield and quality are shown in Figure III.10, whilst those for potato yield and tomato yield and quality are shown in Figure III.11.

Table III.10: *POD_6SPEC critical levels (CL) for crops.*

Species	**Effect parameter**	**Biogeo-graphi-cal region***	**Potential effect at CL (% reduction)**	**Critical level (mmol m^{-2} PLA)****	**Ref10 POD_6 (mmol m^{-2} PLA)**	**Potential maximum rate of reduction (%) per mmol m^{-2} PLA of POD_6SPEC*****
Wheat	Grain yield	A,B,C,M (S,P)*****	5%	1.3	0.0	3.85
Wheat	1000-grain weight	A,B,C,M (S,P)*****	5%	1.5	0.0	3.35
Wheat	Protein yield	A,B,C,M (S,P)*****	5%	2.0	0.0	2.54
Potato	Tuber yield	A,B,C (M,S,P)	5%	3.8	0.0	1.34
Tomato	Fruit yield	M (A,B, C,S,P)	5%	2.0	0.0	2.53
Tomato	Fruit quality	M (A,B, C,S,P)	5%	3.8	0.0	1.30

** A = Atlantic, B = Boreal, C = Continental, M = Mediterranean, P = Pannonian, S = Steppic; Derived for regions not in brackets, but could also be applied to regions in brackets.*

*** Represents the (POD_6SPEC – Ref10 POD_6SPEC) required for a 5% reduction;*

**** Calculate the % reduction using the following formula:*

*(POD_6SPEC – Ref10 POD_6SPEC) * potential maximum rate of reduction;*

***** Different parameterisation of DO_3SE applied for Mediterranean and non-Mediterranean regions.*

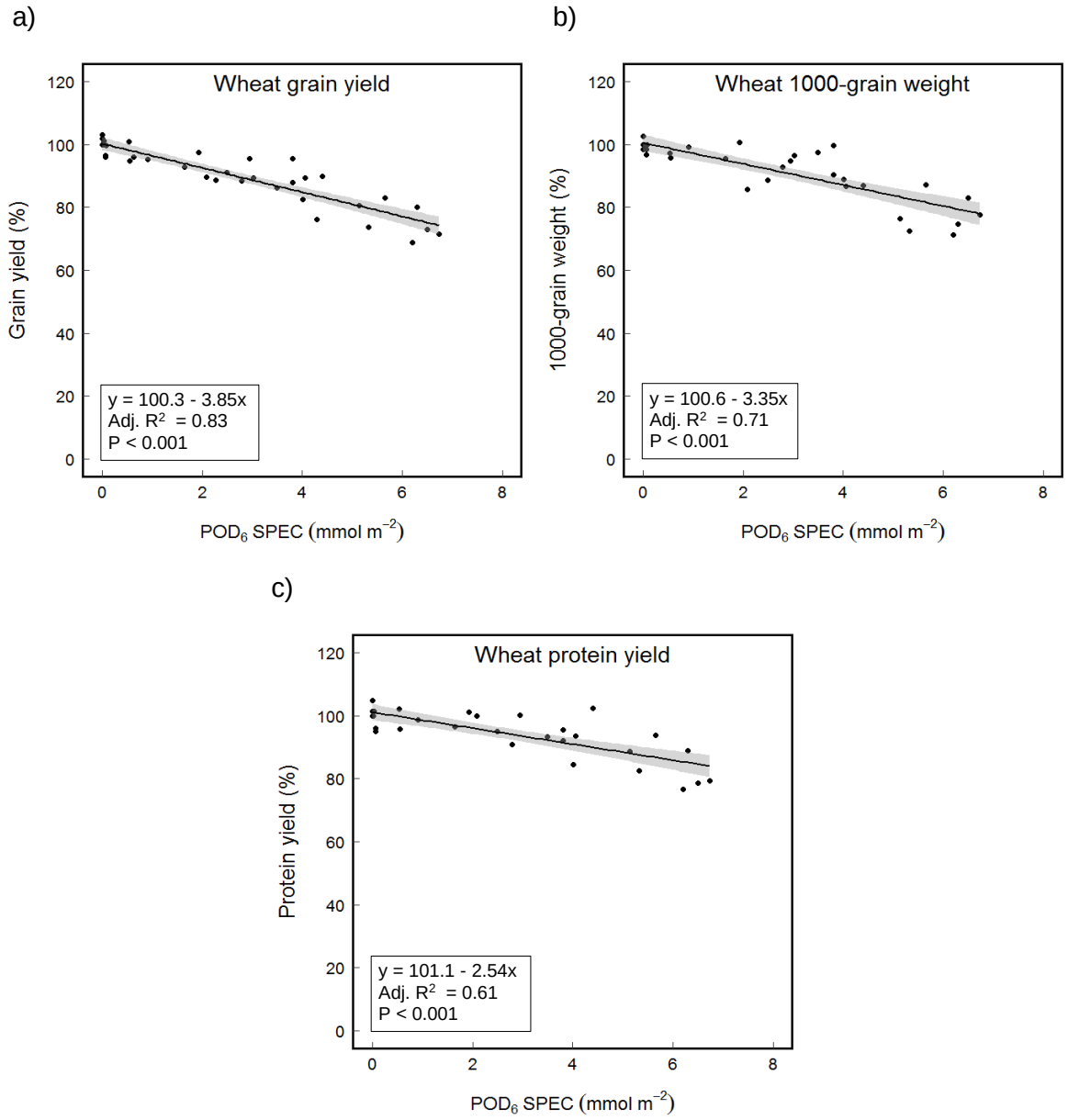

Figure III.10: *The relationship between the percentage yield of wheat and stomatal O_3 flux (POD_6SPEC) for the wheat flag leaf based on five wheat cultivars from three or four European countries (Belgium, Finland, Italy, Sweden): a) grain yield, b) 1000-grain weight, and c) protein yield. The grey area indicates the 95%-confidence interval (Grünhage et al., 2012).*

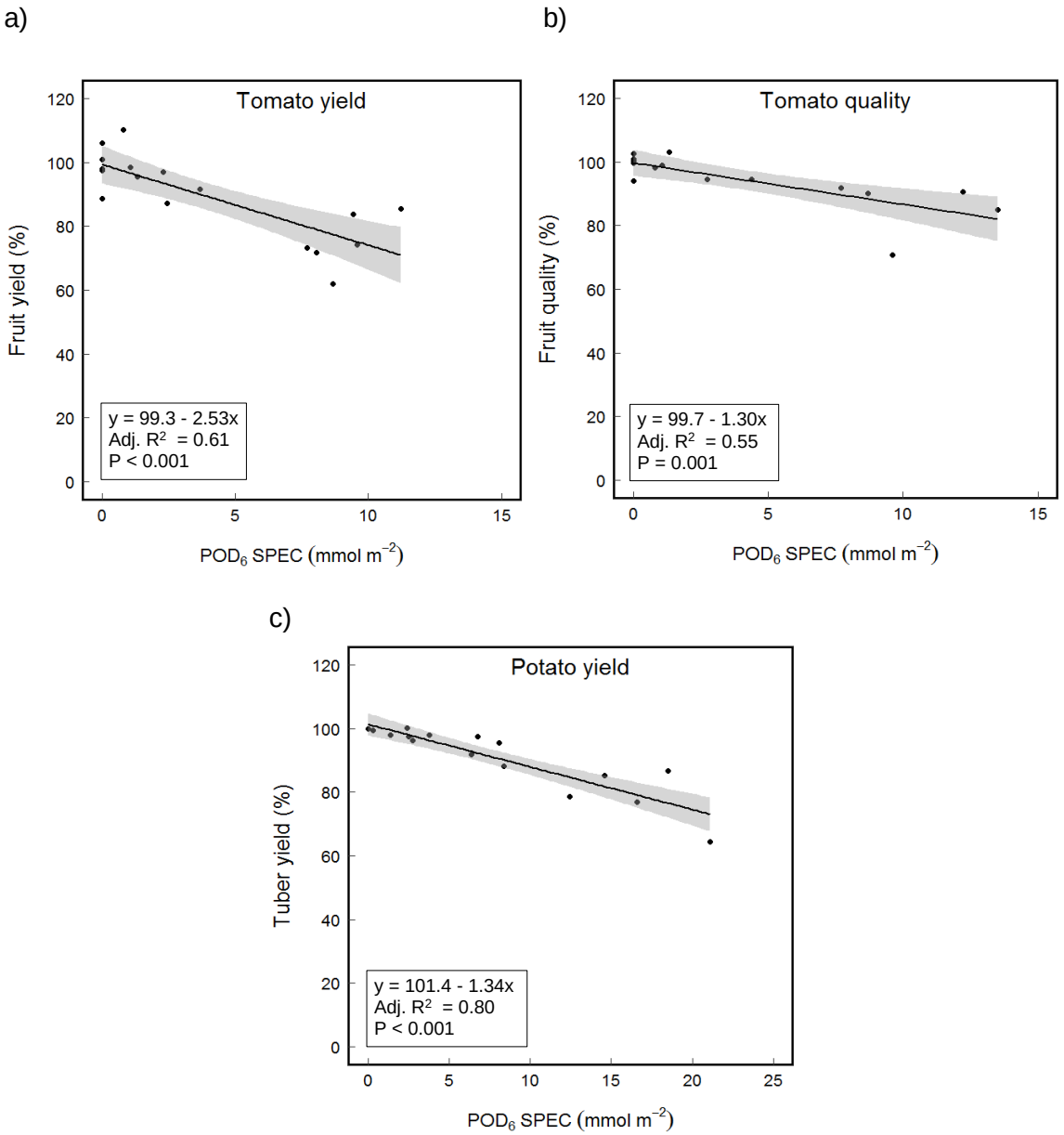

Figure III.11: *The relationship between the percentage a) tomato fruit yield and b) tomato fruit quality and POD_6SPEC for sunlit leaves (González-Fernández et al., 2014) based on data from Italy and Spain, and c) tuber yield of potato and POD_6SPEC for sunlit leaves (Pleijel et al., 2007) based on data from Belgium, Finland, Germany, Sweden. The grey area indicates the 95%-confidence interval.*

III.3.5.3 FOREST TREES

III.3.5.3.1 *PARAMETERISATION OF THE O_3 STOMATAL FLUX MODEL FOR FOREST TREES*

Species-specific stomatal flux-based critical levels are available for non-Mediterranean beech/birch (combined; *Fagus sylvatica/Betula pendula*) and Norway spruce (*Picea abies*), Mediterranean deciduous oak species (*Quercus faginea, Q. pyrenaica and Q. robur*) and Mediterranean evergreen species (*Pinus halepensis*, *Quercus ilex, Q. ballota, Ceratonia*

siliqua). The parameterisation of these flux models is provided in Table III.11 and is based on data from mature trees species, except for Mediterranean deciduous oak species. Parameterisation of the DO_3SE model using data from young oak tree species was considered to better represent risk assessment of deciduous trees in Mediterranean areas than the previous parameterisation based on mature Mediterranean beech. Information on the sources of these parameterisations is summarised in Annex III.3 (Table A.3) and SBD-A and available in detail in Büker et al. (2015; trees in non-Mediterranean regions of Europe), Marzuoli et al. (in prep., Mediterranean broadleaf deciduous species) and Alonso et al. (in prep., Mediterranean evergreen species).

A uniform O_3 flux threshold of Y = 1 nmol m^{-2} s^{-1} PLA was adopted for use in POD_YSPEC for all tree species at the O_3 Critical Levels workshop in Madrid, November 2016, based on data and analyses as presented in Büker et al. (2015). For the majority of tree species, this threshold fulfilled the recommendations that the confidence interval of the intercept includes 100% and that the R^2 value is within 2% of the maximum R^2 value (Büker et al., 2015).

For forest trees, the following additional information is required for calculating stomatal flux using the method provided in Section III.3.4.3 and the parameterisation provided in Table III.11.

Start (A_{start}) and end (A_{end}) of flux accumulation period

POD_1SPEC is accumulated between the start and end of the growing season. For all main receptor species, the start of the growing season is assumed to be equivalent to the start of the flux accumulation period (A_{start}) and is defined as the date of budburst/ leaf emergence or the release of winter dormancy. For all main receptor species, the end of the growing season is assumed to be equivalent to the end of the flux accumulation period (A_{end}) and is defined as the onset of dormancy. For beech and birch, as well as for Norway spruce in the boreal region, A_{start} is estimated using a simple latitude model where A_{start} occurs at year day 105 at latitude 50°N, and A_{start} will alter by 1.5 days per degree latitude earlier on moving south and later on moving north. A_{end} is estimated as occurring at year day 297 at latitude 50°N, and A_{end} will alter by 2 days per degree latitude earlier on moving north and later on moving south. Leaf discolouration is assumed to occur 20 days prior to dormancy and is assumed to be the point at which f_{phen} will start to decrease from g_{max}. Between the onset of dormancy and leaf fall, g_{sto} will be assumed to be zero. The effect of altitude on phenology is incorporated by assuming a later A_{start} and earlier A_{end} by 10 days for every 1000 m a.s.l.

This latitude model agreed relatively well with ground observations from the Mediterranean (Mediavilla & Escudero, 2003; Aranda et al., 2005; Damesin & Rambal, 1995; Grassi & Magnani, 2005 and the Atlantic (Broadmeadow, pers comm.; Duchemin et al., 1999) and with remotely sensed observations for the whole of Europe (Zhang et al., 2004). The latitude model is used mainly due to its simplicity. It is understood that the modelled timing of deciduous tree budburst, at least in northern Europe, may differ from the observed timing of budburst (SBD-B, Karlsson et al., Braun et al.). Furthermore, the start of the gas exchange of coniferous tree species in northern Europe may occur at dates earlier than predicted by the latitude model (SBD-B, Karlsson et al.). The latitude model is not able to reflect changes in the climate. Hence, it is the aim that the latitude model should be replaced with a methodology that is based on meteorological parameters once a more robust model has been fully developed (SBD-B, Karlsson et al., Braun et al.).

For Norway spruce in the continental region, the growth period is determined by air temperature defined according to the f_{temp} function. The growing season is assumed to occur when air temperatures are between the T_{min} and T_{max} thresholds of the f_{temp} relationships. During such periods there is no limitation on conductance associated with leaf development stage (i.e. f_{phen} = 1).

f_{phen}

For forest trees, a modified formulation for the f_{phen} relationship as given in Equations III.2a-c is used (see below). This method allows the use of a consistent formulation irrespective of whether there is a mid-season dip in f_{phen} (to simulate the effect of mid-season photo-oxidative stress on stomatal conductance). The values in brackets for the phenology function in Table III.11 represent "dummy" values to be used in areas where this mid-season dip does not occur:

when $yd \leq A_{start\_FD}$

(III.23a) $f_{phen} = f_{phen\_a}$

when $A_{start\_FD} < yd \leq f_{phen1\_FD} + A_{start\_FD}$

(III.23b) $f_{phen} = ((1-f_{phen\_a})*((yd- A_{start\_FD})/f_{phen1\_FD})+f_{phen\_a})$

when $f_{phen1\_FD} + A_{start\_FD} < yd \leq LIM_{start\_FD}$

(III.23c) $f_{phen} = f_{phen\_b}$

when $LIM_{start\_FD} < yd < LIM_{start\_FD} + f_{phen2\_FD}$

(III.23d) $f_{phen} = (1-f_{phen\_c}) * (((f_{phen2\_FD} + LIM_{start\_FD}) - (LIM_{start\_FD} + (yd-LIM_{start\_FD}))) /f_{phen2\_FD}) + f_{phen\_c}$

when $LIM_{start\_FD} + f_{phen2\_FD} \leq yd \leq LIM_{end\_FD} - f_{phen3\_FD}$

(III.23e) $f_{phen} = f_{phen\_c}$

when $LIM_{end\_FD} - f_{phen3\_FD} < yd < LIM_{end\_FD}$

(III.23f) $f_{phen} = (1-f_{phen\_c}) * ((yd-(LIM_{end\_FD} - f_{phen3\_FD}))/f_{phen3\_FD}) + f_{phen\_c}$

when $LIM_{end\_FD} \leq yd \leq A_{end\_FD} - f_{phen4\_FD}$

(III.23g) $f_{phen} = f_{phen\_d}$

when $A_{end\_FD} - f_{phen4\_FD} < yd < A_{end\_FD}$

(III.23h) $f_{phen} = (1-f_{phen\_e}) * ((A_{end\_FD}-yd) / f_{phen4\_FD}) + f_{phen\_e}$

when $yd \geq A_{end\_FD}$

(III.23i) $f_{phen} = f_{phen\_e}$

Table III.11: *Summary of the parameterisation of the DO_3SE model for POD_1SPEC calculations of sunlit leaves at the top of the canopy of individual tree species or groups of tree species growing in Europe. Note: Further region- and species-specific parameterisations for species can be found in SBD-A and SBD-B.*

Parameter	**Units**	**Forest tree species parameterisation - POD_1SPEC**					
Region *(may also be applicable in these regions)*		Boreal		Continental *(Atlantic, Steppic, Pannonian)*		Mediterranean	
Forest type		Coniferous	Broadleaf deciduous	Coniferous	Broadleaf deciduous	Broadleaf deciduous	Evergreen
Tree species	Common name	**Norway spruce**	**Silver birch**	**Norway spruce**	**Beech**	**Deciduous oak species[i, ii]**	**Evergreen species[iii]**
	Latin name	*Picea abies*	*Betula pendula*	*Picea abies*	*Fagus sylvatica*		
g_{max}	mmol O_3 m^{-2} PLA s^{-1}	125	240	130	155	265	195

f_{min}	fraction	0.1	0.1	0.16	0.13	0.13	0.02
light_a	-	0.006	0.0042	0.01	0.006	0.006	0.012
T_{min}	°C	0	5	0	5	0	1
T_{opt}	°C	20	20	14	16	22	23
T_{max}	°C	200[iv]	200[iv]	35	33	35	39
VPD_{max}	kPa	0.8	0.5	0.5	1.0	1.1	2.2
VPD_{min}	kPa	2.8	2.7	3.0	3.1	3.1	4.0
ΣVPD_{crit}	kPa	-	-	-	-	-	-
PAW_t	%	-	-	-	-	-	-
SWC_{max}[v]	% volume	15	15	-	-	-	-
SWC_{min}[v]	% volume	1	1	-	-	-	-
SWP_{max}	MPa	-	-	-0.05	-0.05	-1.0	-1.0
SWP_{min}	MPa	-	-	-0.5	-1.25	-2.0	-4.5
f_{O3}	fraction	-	-	-	-	-	-
A_{start}_FD	day of year	Latitude model	Latitude model	f_{temp}[vi]	Latitude model	Latitude model	1 (Jan 1)
A_{end}_FD	day of year	Latitude model	Latitude model	f_{temp}[vi]	Latitude model	Latitude model	365 (Dec 31)
Leaf dimension	cm	0.8	5.0	0.8	7.0	4.2	3
Canopy height	m	20	20	20	25	20	20
f_{phen_a}	fraction	0.0	0.0	0.0	0.0	0.3	1.0
f_{phen_b}	fraction	(1.0)	(1.0)	(1.0)	(1.0)	(1.0)	(1.0)
f_{phen_c}	fraction	1.0	1.0	1.0	1.0	1.0	0.3
f_{phen_d}	fraction	(1.0)	(1.0)	(1.0)	(1.0)	(1.0)	(1.0)
f_{phen_e}	fraction	0.0	0.0	0.0	0.4	0.3	1.0
$f_{phen\_1\_FD}$	no. of days	20	20	0	20	15	(0)
$f_{phen\_2\_FD}$	no. of days	(200)	(200)	(200)	(200)	(200)	130
$f_{phen\_3\_FD}$	no. of days	(200)	(200)	(200)	(200)	(200)	60
$f_{phen\_4\_FD}$	no. of days	30	30	0	20	20	(0)
LIM_{start_FD}	year day	(0.0)	(0.0)	(0.0)	(0.0)	(0.0)	80 (Mar 21)
LIM_{end_FD}	year day	(0.0)	(0.0)	(0.0)	(0.0)	(0.0)	320 (Nov 16)

The values in brackets represent "dummy" values required for DO_3SE modelling purposes. "-" = parameterisation not required for this species.

[i] *Mediterranean deciduous oak are represented here by Quercus robur, Q. pyrenaica and Q. faginea. Only for these tree species the parameterisation is based on young trees (Marzuoli, in prep.).*

[ii] *Local species-specific parameterisations can be found in scientific background document A (SBD-A).*

[iii] *Mediterranean evergreen species are represented here by the parameterisation for adult Quercus ilex trees.*

[iv] *The T_{max} value is set at 200 °C to simulate the weak response to high temperatures of Norway spruce and birch trees growing under Northern European conditions (the stomatal response is instead mediated by high VPD values). Hence, the T_{max} value should be viewed as a forcing rather than descriptive parameter.*

[v] *Soil water content (SWC) is calculated as the soil water content available for transpiration, i.e. the actual SWC minus the SWC at the wilting point.*

[vi] *For continental Norway spruce, the growing season is assumed to occur when air temperatures are between the T_{min} and T_{max} thresholds of the f_{temp} relationships. Actual data are recommended if available!*

III.3.5.3.2 *FLUX-EFFECT RELATIONSHIPS AND CRITICAL LEVELS FOR FOREST TREES*

Box 7: Applications for species-specific (POD_1SPEC) flux-effect relationships and critical levels for forest trees

The species- group or species-specific flux models, associated response functions and critical levels for forest trees were derived from experiments with young trees and can be used to quantify the potential negative impacts of O_3 on the annual growth of the living biomass of trees at the local and regional scale. They can be used as a starting point for calculation of impacts on carbon sequestration and tree diversity.

The applications of the POD_YSPEC functions and critical levels for forest trees are described in Box 7. Methods are currently being developed for quantifying O_3 impacts on tree growth rates, such as the Net Annual Increment (NAI; SBD-B, Büker et al.). When developed, such methods should be applied to assess O_3 impacts over the entire rotation periods of trees. Flux models have been developed for the effects of O_3 on individual tree species in one year. Where effects were reported over more than one year in experiments, the mean flux was determined by dividing the total by the number of years of O_3 exposure. Based on the exponential nature of the growth of young trees, the following procedure was applied for the correction of the biomass change in multiannual experiments:

(III.24) $$biom_{yr} = biom^{\frac{1}{years}}$$

where $biom_{yr}$ is the corrected biomass, biom is the biomass in fractions of the control and years is the duration of the experiment in years.

The critical levels for forest trees were set to values for an acceptable biomass loss. Critical levels have been derived for either a 2% (Norway spruce) or a 4% (beech/birch, Mediterranean deciduous oaks and Mediterranean evergreen species) reduction in annual new growth (based on above ground, root or whole tree biomass) of young trees of up to 10 years of age. For each species, data was from independent experiments conducted in: two countries with three species for Mediterranean deciduous oaks; one country with four species for Mediterranean evergreen; two countries with one species for Norway spruce; and three countries with two species for beech and birch (combined in one function) (see Annex 3, Table A2). Critical levels were determined based on the slope of the flux-effect relationship and are summarised in Table III.12.

Table III.12: *POD_1SPEC critical levels (CL) for forest tree species.*

Species	**Effect parameter**	**Biogeo-graphi-cal region***	**Potential effect at CL (% annual reduc-tion)**	**Critical level (mmol m^{-2} PLA)****	**Ref10 POD_1 (mmol m^{-2} PLA)**	**Potential maximum rate of reduction (%) per mmol m^{-2} PLA of POD_1SPEC*****
Beech and birch	Whole tree biomass	B,C (A,S,P)	4%	5.2	0.9	0.93
Norway spruce	Whole tree biomass	B,C (A,S,P)	2%	9.2	0.1	0.22

Med. deciduous oaks	Whole tree biomass	M	4%	14.0	1.4	0.32
Med. deciduous oaks	Root biomass	M	4%	10.3	1.4	0.45
Med. evergreen	Above-ground biomass	M	4%	47.3	3.5	0.09

* *A: Atlantic; B: Boreal; C: Continental, S: Steppic, P: Pannonian; M: Mediterranean. Derived for regions not in brackets, but could also be applied to regions in brackets.*

*** Represents the (POD_1SPEC – Ref10 POD_1SPEC) required for a x% reduction*

**** Calculate the % reduction using the following formula:*

*(POD_1SPEC – Ref10 POD_1SPEC) * potential maximum rate of reduction.*

The flux-effect relationships for individual tree species or groups of tree species are shown in Figure III.12.

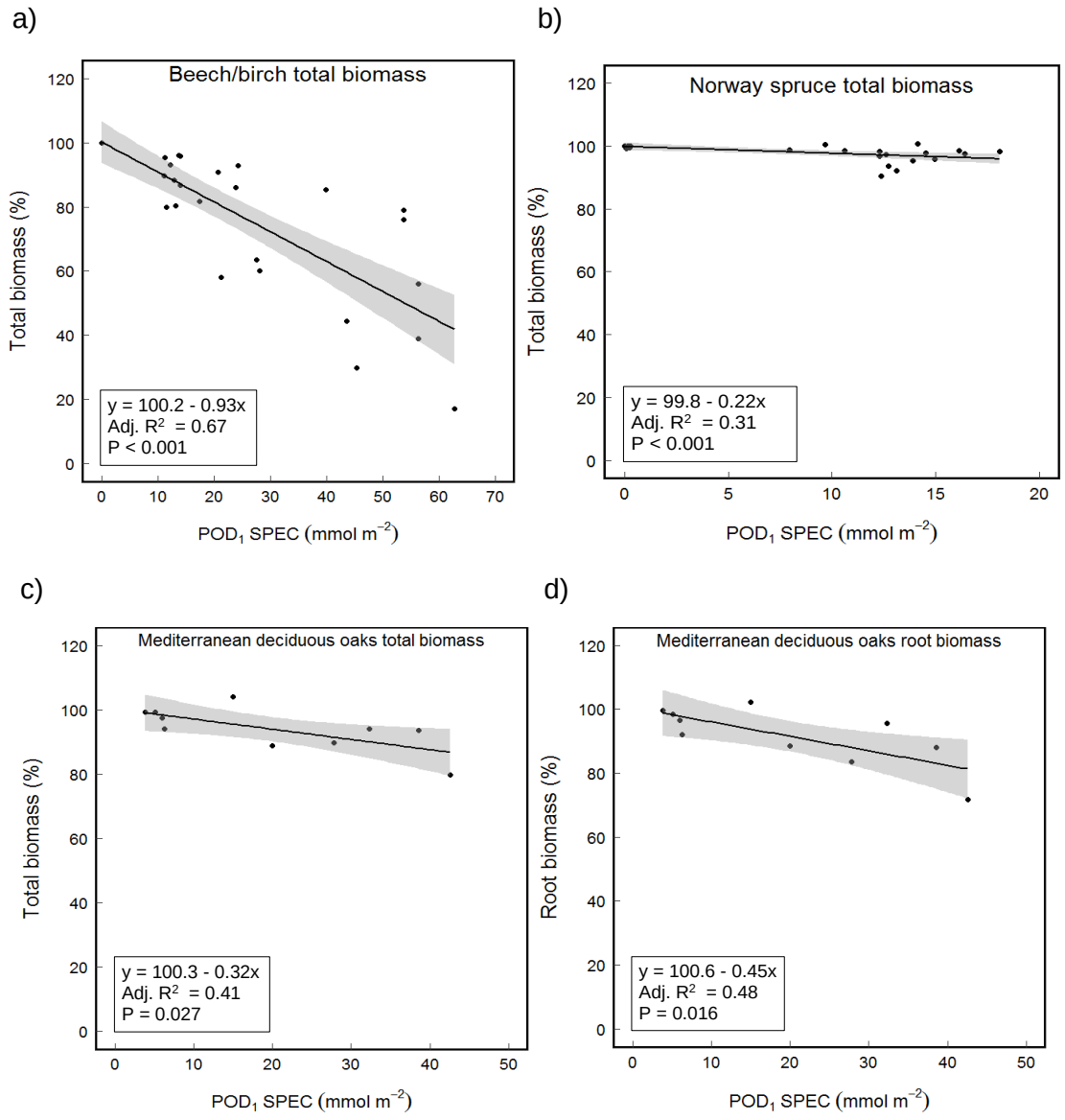

e)

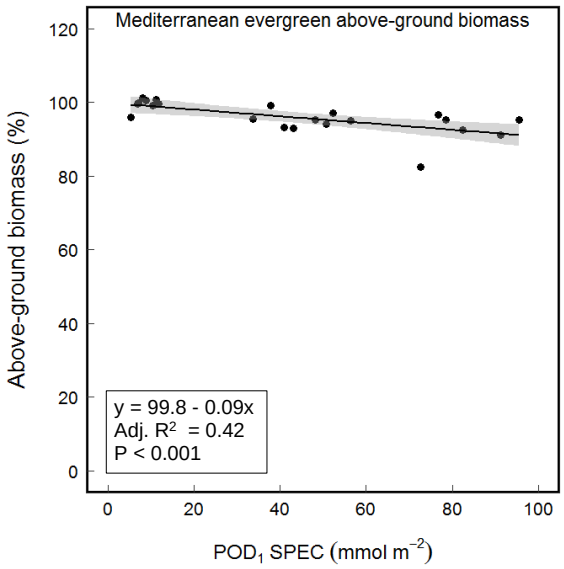

Figure III.12: The relationship between the percentage total biomass and the stomatal O_3 flux (POD_1SPEC) for sunlit leaves of a) beech (Fagus sylvatica) and silver birch (Betula pendula) based on data from Finland, Sweden and Switzerland (Büker et al., 2015), b) Norway spruce (Picea abies) based on data from France, Sweden and Switzerland (Büker et al., 2015), c) Mediterranean deciduous oak based on data from Italy and Spain (Calatayud et al., 2011; Marzuoli et al., 2016, in prep.), d) between the percentage root biomass and the stomatal O_3 flux (POD_1SPEC) for sunlit leaves of Mediterranean oak (Calatayud et al., 2011; Marzuoli et al., 2016, in prep.), and e) between the percentage of above-ground biomass and the stomatal O_3 flux (POD_1SPEC) for sunlit leaves of Mediterranean evergreen species based on data from Spain (Alonso et al., in prep). The grey area indicates the 95%-confidence interval.

III.3.5.4 (SEMI-)NATURAL VEGETATION

III.3.5.4.1 *CHOICE OF REPRESENTATIVE SPECIES AND ECOSYSTEMS*

The (semi-)natural vegetation type includes all vegetation not planted by humans, excluding forests, but influenced deliberately or inadvertently by human actions (Di Gregorio & Jansen, 2000). This vegetation type is the most florally diverse of those considered - there are 4000+ species of (semi-)natural vegetation in Europe – making the generalisations needed for setting critical levels difficult. Although response functions and relative sensitivities have been derived for >100 species (Hayes et al., 2007; Bergmann et al., 2015), at least 98 % of (semi-)natural species remain untested.

Due to the large diversity of (semi-)natural vegetation communities across Europe in terms of ecophysiology, life form, management practices such as grazing, cutting or fertilization regime or species composition, O_3 critical levels have been established for widespread O_3 sensitive species representing broad categories of (semi-)natural vegetation plant communities. Critical levels have been established for:

- **Temperate perennial grasslands** found in Boreal**,** Atlantic and Continental biogeographical regions of Europe that are dominated by grasses and forbs and have little or no tree cover, and may be grazed. The majority of vegetation species are perennials, but annual species may also be present**.** Parameterisations and critical levels for temperate perennial grasslands may also be applicable for

Pannonian and Steppic regions, but this has not been tested yet and stronger soil water limitations might be expected.

- **Mediterranean annual pastures** that are dominated by annual plants (grasses and forbs, including legumes). They include Dehesa annual pastures and other grazed annual pastures found in the Mediterranean region of Europe.

Information from field experiments to date indicates that subalpine grassland vegetation is moderately tolerant to current ambient O_3 concentrations (Bassin et al., 2013, 2015; Volk et al., 2014). Hence, O_3 critical levels have not been established for (sub)alpine grassland communities. Currently there is insufficient data to establish a flux-based O_3 critical level for other (semi-)natural vegetation communities.

Only experiments conducted in Europe under semi-controlled conditions have been considered for critical level derivation, in which the selected species were growing in competition with other grassland species (Temperate perennial grasslands) and as single species or two-species mixtures (Mediterranean annual species) and subjected to different fertilization and cutting regimes. Several independent experiments have been included in each function.

III.3.5.4.2 *PARAMETERISATION OF THE O_3 STOMATAL FLUX MODEL FOR (SEMI-)NATURAL VEGETATION*

Parameterisations of the DO_3SE model for representative species of (semi-)natural vegetation are shown in Table III.13. For **temperate perennial grasslands** it is recommended to use the forbs parameterisation as an indicator of a general risk to grassland habitats. The grass parameterisation can be used to specifically assess the risk for grass species. For **Mediterranean annual pastures** it is recommended to use the legumes parameterisation as an indicator of a general risk to annual pasture habitats.

Time window

Time windows are “default” parameters that should be adjusted by the user if more appropriate local information is available. Select the accumulation period that gives the highest flux or is the most suitable season.

Canopy height

Default values are provided for general application.

EUNIS classifications

The most suitable EUNIS classes (http://eunis.eea.europa.eu/) to use are those represented by the habitats for which the critical levels have been derived:

Temperate perennial grassland:

- E2.1 Permanent mesotrophic pastures and aftermath-grazed meadows;
- E2.2 Low and medium altitude hay meadows;
- E2.7 Unmanaged mesic grassland;
- E2.5 Meadows of the steppe zone.

Mediterranean annual pasture:

- E1.3 Mediterranean xeric grassland;
- E1.6 Subnitrophilous annual grassland;
- E1.8 Closed Mediterranean dry acid and neutral grassland;
- E7.3 Dehesa.

Table III.13: *Parameterisation of the DO_3SE model for POD_1SPEC calculations for sunlit leaves at the top of the canopy for representative O_3-sensitive (semi-)natural vegetation species.*

Parameter	Units	(Semi-)natural vegetation parameterisation for sunlit leaves at top of canopy - POD_1SPEC		
Region *(may also be applicable in these regions)*		Atlantic, Boreal, Continental, *(Pannonian, Steppic)*	Atlantic, Boreal, Continental, *(Pannonian, Steppic)*	Mediterranean
Land cover type		Perennial grasslands (Grass spp.)	Perennial grasslands (Forbs incl. legumes)	Annual pastures (Legume spp.)
g_{max}	mmol O_3 m^{-2} PLA s^{-1}	190	210	782
f_{min}	fraction	0.1	0.1	0.02
light_a	-	0.01	0.02	0.013
T_{min}	°C	10	10	8
T_{opt}	°C	24	22	22
T_{max}	°C	36	36	33
VPD_{max}	kPa	1.75	1.75	2.2
VPD_{min}	kPa	4.5	4.5	4.3
ΣVPD_{crit}	kPa	-	-	_
PAW_t	%	-	-	-
SWC_{max}	% volume	-	-	18.3
SWC_{min}	% volume	-	-	0.03
SWP_{max}	MPa	-0.1	-0.1	-
SWP_{min}	MPa	-1	-0.6	-
f_{O3}	fraction	-	-	-
$A_{start}\_FD^i$	day of year	91 (April 1st)	91 (April 1st)	32 (February 1st)
$A_{end}\_FD^i$	day of year	273 (September 30th)	273 (September 30th)	181 (June 30th)
Time window length	month	3	3	1.5
Leaf dimension	cm	2[ii]	4[ii]	2
Canopy height	m	0.2	0.2	0.2
f_{phen_a}	fraction	1	1	1
f_{phen_b}	fraction	1	1	1
f_{phen_c}	fraction	1	1	1
f_{phen_d}	fraction	1	1	1
f_{phen_e}	fraction	1	1	1
$f_{phen\_1\_FD}$	no. of days	-	-	-
$f_{phen\_2\_FD}$	no. of days	-	-	-
$f_{phen\_3\_FD}$	no. of days	-	-	-
$f_{phen\_4\_FD}$	no. of days	-	-	-
LIM_{start_FD}	year day	-	-	-
LIM_{send_FD}	year day	-	-	-

"-" = parameterisation not required for this species.

[i] *Days of year given for non-leap year.*

[ii] *Not given, set to match wheat (grass species) and potato (forb species, including legumes).*

III.3.5.4.3 *FLUX-EFFECT RELATIONSHIPS AND CRITICAL LEVELS FOR (SEMI-)NATURAL VEGETATION*

Box 8: Applications for species-specific (POD_1SPEC) flux-effect relationships and critical levels for (semi-) natural vegetation

The species-group specific flux models, associated response functions and critical levels for (semi-)natural vegetation were derived from experiments with O_3-sensitive species grown in competition (Temperate perennial grasslands) or as single species and two-species mixtures (Mediterranean annual pastures). Response functions and critical levels can be used to quantify the risk of potential negative O_3 impacts on biomass and reproductive capacity. They can be used as a starting point for calculation of impacts on carbon sequestration and plant biodiversity.

The applications of the POD_YSPEC functions and critical levels for (semi-)natural vegetation are described in Box 8. For (semi-)natural vegetation, a flux-threshold Y of 1 nmol m^{-2} s^{-1} (POD_1SPEC) was used. This threshold fulfilled the recommendations made by Büker et al. (2015), i.e. that the confidence interval of the intercept includes 100% and that the R^2 value is within 2% of the maximum R^2 value, and matches the one used for forest trees.

Table III.14: *POD_1SPEC critical levels (CL) for O_3 sensitive (semi-)natural vegetation.*

Species	**Effect parameter**	**Biogeographical region***	**Potential effect at CL (% reduction)**	**Critical level (mmol m^{-2} PLA)****	**Ref10 POD_1 (mmol m^{-2} PLA)**	**Potential maximum rate of reduction (%) per mmol m^{-2} PLA of POD_1SPEC*****
Temperate perennial grassland	Above-ground biomass	A, B,C (S,P)	10%	10.2	0.1	0.99
Temperate perennial grassland	Total biomass	A, B,C (S,P)	10%	16.2	0.1	0.62
Temperate perennial grassland	Flower number	A, B,C (S,P)	10%	6.6	0.1	1.54
Med. annual pasture	Above-ground biomass	M	10%	16.9	5.2	0.85
Med. annual pasture	Flower/ seed biomass	M	10%	10.8	4.6	1.61

* *A: Atlantic; B: Boreal; C: Continental, S: Steppic, P: Pannonian; M: Mediterranean. Derived for species growing in regions not in brackets, but could also be applied to regions in brackets.*

*** Represents the (POD_1SPEC – Ref10 POD_1SPEC) required for a x% reduction*

**** Calculate the % reduction using the following formula:*

*(POD_1SPEC – Ref10 POD_1SPEC) * potential maximum rate of reduction.*

A 10% reduction in the effects parameter was considered to be an important effect that could change ecosystem dynamics. Hence, critical levels were determined for a 10% reduction of the effect based on the slope of the relationship and are summarised in Table III.14. The flux-effect relationships for (semi-)natural vegetation are shown in Figures III.13 and III.14 and further details can be found in Annex 3, Table A.4. It should be noted that the critical levels and response functions were derived from experimental data in Europe. Two sets of critical levels are provided per habitat reflecting O_3 impacts on growth or reproductive output. Users should select the most appropriate response for their requirements. POD_YSPEC-based critical levels can be used to assess the potential risk of O_3 impacts on the biomass and vitality of (semi-)natural vegetation species. These critical levels may also protect against loss of plant biodiversity, but this has not yet been confirmed.

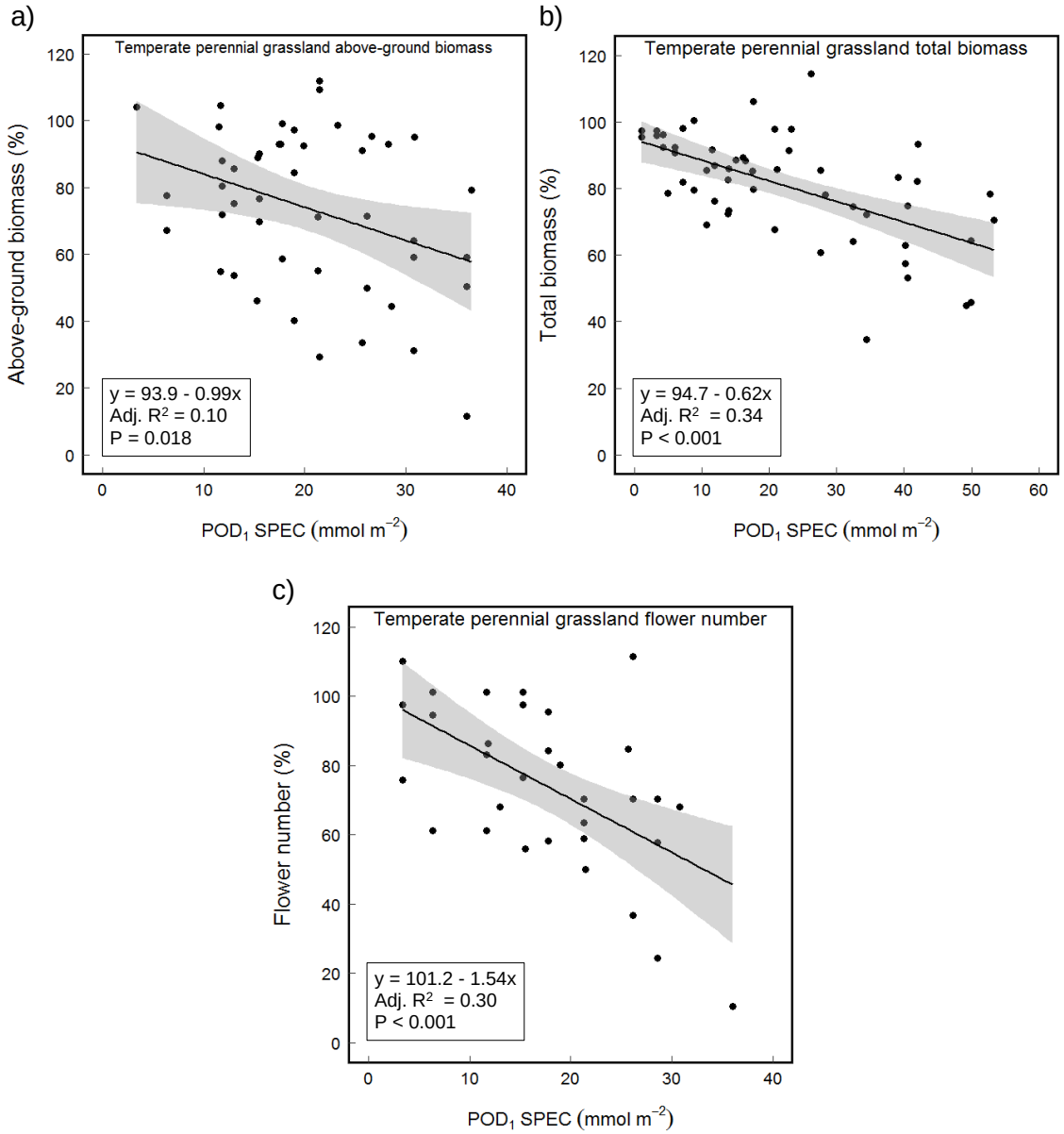

Figure III.13: *The relationship between the stomatal O_3 flux (POD_1SPEC) for sunlit leaves and percentage a) above-ground biomass, b) total biomass and c) flower number of temperate perennial grasslands. The grey area indicates the 95%-confidence interval. Data are from experiments conducted in the UK (Hayes et al., 2011, 2012, Hewitt et al., 2014, Wagg et al., 2012, Wyness et al., 2011 and unpublished data peer-reviewed at the Madrid Workshop, 2016).*

The flux models and critical levels are the most applicable to areas where the vegetation is similar to the species/vegetation type for which a flux-based critical level has been derived (see suitable EUNIS classifications above). For other (semi-)natural vegetation communities the critical levels only provide an indication of a relative risk to these communities, except for Alpine grasslands and pastures which are rather resilient to ozone in terms of biomass growth (Volk et al., 2014).

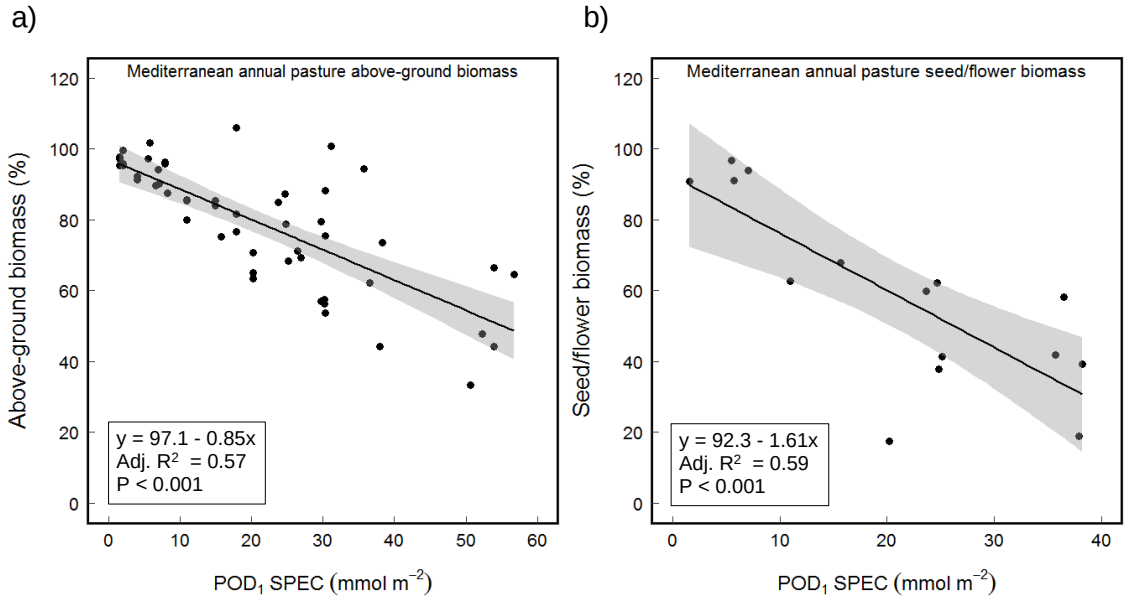

Figure III.14: *The relationship between the stomatal O_3 flux (POD_1SPEC) for sunlit leaves and percentage a) aboveground biomass and b) seed/flower biomass of Mediterranean annual pastures. The grey area indicates the 95%-confidence interval. Data are from experiments conducted in Spain (Gimeno et al., 2004a,b; Sanz et al., 2005, 2007, 2014, 2016).*

III.3.6 VEGETATION-SPECIFIC FLUX-EFFECT RELATIONSHIPS AND CRITICAL LEVELS FOR ASSESSING RISK IN LARGE-SCALE INTEGRATED ASSESSMENT MODELLING (USING POD_YIAM)

III.3.6.1 APPLICATIONS

The simplified flux models (POD_YIAM) and associated response functions and critical levels described in this section **are for use in integrated assessment modelling (IAM)** at European, regional and potentially global scale for similar biogeographic regions. Using POD_YIAM, the degree of risk of damage within large scale modelling, including scenario analysis and optimisation runs within the GAINS model (**G**reenhouse Gas and **A**ir Pollution **In**teractions and **S**ynergies) can be determined by using simplified parameterisations to represent vegetation types. POD_YIAM flux models provide an **indicative risk assessment** and are less robust than POD_YSPEC flux models. They can be applied to assess exceedance of critical levels and/or to quantify the risk of adverse O_3 impacts for the most sensitive vegetation under the worst case scenario (Box 9).

Separate simplified flux models, associated response relationships and critical levels have been defined for crops, forest trees and (semi-)natural vegetation, with parameterisations provided for Mediterranean and non-Mediterranean areas.

Text Box 9: Applications for vegetation-type flux models and critical levels, POD_YIAM

These flux models have simpler form than POD_YSPEC and have been developed specifically for use in large-scale integrated assessment modelling, including for scenario analysis and optimisation runs. Separate parametrisations are provided for Mediterranean and non-Mediterranean areas for application in risk assessments for crops, forest trees and (semi-)natural vegetation.

The flux-effect relationships can be used for:

- **Crops:** potential maximum yield loss calculation and indicative economic losses in worst case scenario;
- **Forest trees and (semi-)natural vegetation:** indicative of the potential maximum risk for estimating environmental cost, but not economic losses.

The critical levels can be used for calculating critical levels exceedances, both amount and area. For applications in a climate change context, the POD_YSPEC method is recommended as key factors such as phenology and soil moisture are not included in the parameterisation of POD_YIAM.

III.3.6.2 POD_YIAM-BASED FLUX-EFFECT RELATIONSHIPS AND CRITICAL LEVELS FOR CROPS, FOREST TREES AND GRASSLANDS/PASTURE

III.3.6.2.1 *PARAMETERISATION OF THE O_3 STOMATAL FLUX MODEL (POD_YIAM)*

The simplified flux models suitable for IAM do not include the modifying effect of soil moisture and phenology (and O_3 in the case of crops) on the stomatal conductance, hence f_{SW} and f_{phen} (and f_{O3} for crops) are set to 1 between the start and the end of the accumulation period. Using the simplified flux models as a stand-alone application, this method would indicate the risk of O_3 damage under the worst case scenario where soil moisture is not limiting stomatal O_3 flux. However, when used within the EMEP model (Simpson et al., 2012), a simplified soil moisture index is included and further work is ongoing to optimise the applicability of the soil moisture index in soil moisture limited areas or under scenarios of climate change. The parameterisations for POD_YIAM are provided in Table III.15.

Crops

For crops, the parameterisation for the POD_YIAM flux model is based on wheat, a sensitive crop for which abundant information exists (Table III.15). Due to difficulties in estimating the O_3 flux using Y = 6 nmol m^{-2} s^{-1} in large scale modelling and IAM arising from the strong increase in the uncertainty in modelled POD with increasing Y, Y= 3 nmol m^{-2} s^{-1} is to be used (POD_3IAM). To accommodate the need for IAM to use a longer time period than the thermal time–based time window used for POD_6SPEC, POD_3IAM is accumulated over 90 days, centred on the timing of mid-anthesis (flowering) in wheat (see Section III.3.5.2).

Forest trees

For forest trees, the parameterisation for the POD_1IAM flux models has been developed from the POD_1SPEC models for non-Mediterranean broadleaf deciduous species (beech - *Fagus sylvatica*, birch - *Betula pendula,* temperate oak - *Quercus petraea* and *Q. robur,* and poplar - *Populus spp.)* and Mediterranean broadleaf deciduous species (*Quercus faginea, Q. robur and Q. pyrenaica*). For the derivation of a flux-effect relationship, a Y value of 1 nmol m^{-2} s^{-1}

Table III.15: *Parameterisation of the DO_3SE model for POD_YIAM calculations for the flag leaves/sunlit leaves at the top of the canopy for crops, forests and (semi-) natural vegetation. Separate parameterisations are provided for Mediterranean and non-Mediterranean areas.*

Parameter	Units	Crop parameterisation POD_3IAM		Forest trees parameterisation POD_1IAM		(Semi-)natural vegetation parameterisation POD_1IAM	
Biogeographic region		**Atlantic, Boreal, Continental, Steppic, Pannonian**	**Mediterranean**	**Atlantic, Boreal, Continental, Steppic, Pannonian**	**Mediterranean**	**Atlantic, Boreal, Continental, Steppic, Pannonian**	**Mediterranean**
Based on species		**Wheat**	**Wheat**	**Beech, birch, temperate oak, poplar**	**Deciduous oak spp.**	**O_3-sensitive forbs, including legumes**	**O_3-sensitive legumes**
g_{max}	mmol O_3 m^{-2} PLA s^{-1}	500	430	150	265	210	782
f_{min}	fraction	0.01	0.01	0.1	0.13	0.1	0.02
light_a	-	0.0105	0.0105	0.006	0.006	0.02	0.013
T_{min}	°C	12	13	0	0	10	8
T_{opt}	°C	26	28	21	22	22	22
T_{max}	°C	40	39	35	35	36	33
VPD_{max}	kPa	1.2	3.2	1.0	1.1	1.75	2.2
VPD_{min}	kPa	3.2	4.6	3.25	3.1	4.5	4.3
ΣVPD_{crit}	kPa	8	8	-	-	-	_
PAW_t	%	$f_{SW} = 1$	$f_{SW} = 1$	-	-	-	-
SWC_{max}	% volume	-	-	-	-	-	-
SWC_{min}	% volume	-	-	-	-	-	-
SWP_{max}	MPa	-	-	$f_{SW} = 1$	$f_{SW} = 1$	$f_{SW} = 1$	$f_{SW} = 1$
SWP_{min}	MPa	-	-	$f_{SW} = 1$	$f_{SW} = 1$	$f_{SW} = 1$	$f_{SW} = 1$
f_{O3}	fraction	1	1	-	-	-	-
A_{start}_ETS	ºC day	45 days before mid-anthesis in wheat*	45 days before mid-anthesis in wheat*	Latitude model	Latitude model	91 (April 1st)	32 (February 1st)
A_{end}_ETS	ºC day	45 days after mid-anthesis in wheat*	45 days after mid-anthesis in wheat*	Latitude model	Latitude model	273 (September 30th)	181 (June 30th)
Time window length	month	-	-	-	-	3	1.5
Leaf dimension	cm	2	2	7	4.2	4	2
Canopy height	m	1	1	20	20	0.2	0.2

f_{phen_a}	fraction	1.0	1.0	0.0	0.0	1.0	1.0
f_{phen_b}	fraction	1.0	1.0	(1.0)	(1.0)	1.0	1.0
f_{phen_c}	fraction	1.0	1.0	1.0	1.0	1.0	1
f_{phen_d}	fraction	1.0	1.0	(1.0)	(1.0)	1.0	1.0
f_{phen_e}	fraction	1.0	1.0	0.0	0.0	1.0	1.0
$f_{phen\_1\_ETS}$	ºC day	-	-	-	-	-	-
$f_{phen\_2\_ETS}$	ºC day	-	-	-	-	-	-
$f_{phen\_3\_ETS}$	ºC day	-	-	-	-	-	-
$f_{phen\_4\_ETS}$	ºC day	-	-	-	-	-	-
$f_{phen\_5\_ETS}$	ºC day	-	-	-	-	-	-
$f_{phen\_1\_FD}$	no. of days	-	-	15	20	-	-
$f_{phen\_2\_FD}$	no. of days	-	-	(200)	(200)	-	-
$f_{phen\_3\_FD}$	no. of days	-	-	(200)	(200)	-	-
$f_{phen\_4\_FD}$	no. of days	-	-	20	50	-	-
LIM_{start_FD}	year day	-	-	(0.0)	(0.0)	-	-
LIM_{send_FD}	year day	-	-	(0.0)	(0.0)	-	-

The values in brackets represent "dummy" values required for DO_3SE modelling purposes. "-" = parameterisation not required for this species.

** 90d accumulation period, centred on the timing of mid-anthesis in wheat, see Section III.3.5.2.1 for details.*

(POD_1IAM) was used in agreement with POD_1SPEC (see Section III.3.5.3). The start and the end of the accumulation period is still determined by the latitude model.

(Semi-)natural vegetation

For (semi-)natural vegetation, the parameterisation for the POD_1IAM flux models has been developed from the POD_1SPEC models for temperate perennial grasslands, using the parameterisation for forbs (including legumes) and for legumes for Mediterranean annual pasture (see Section III.3.5.4).

III.3.6.2.2 *FLUX-EFFECT RELATIONSHIPS AND CRITICAL LEVELS FOR INTEGRATED ASSESSMENT MODELLING (IAM)*

The critical levels for use with POD_YIAM are shown in Table III.16. These have been derived from response functions based on POD_3IAM for crops, and POD_1IAM for forest trees and (semi-)natural vegetation (Figure III.15). It should be noted that for crops, the function was first derived for datasets based on 45 days (the minimum exposure period in the experiments); the values have been doubled to accommodate the longer 90 day time interval required. For crops, the effect parameter was grain yield, for forest trees it was total biomass and for (semi-)natural vegetation it was flower number (temperate perennial grasslands) or flower/seed biomass (Mediterranean annual pastures).

Table III.16: *POD_YIAM critical levels (CL) for crops, forest trees and (semi-)natural vegetation.*

Vegetation type (POD_YIAM)	**Effect parame-ter**	**Use to assess risk of reduction in**	**Biogeo-graphi-cal region***	**Potential effect at CL (% reduction)**	**Critical level (mmol m^{-2} PLA)****	**Ref10 POD_Y (mmol m^{-2} PLA)**
Crops (POD_3IAM)	Grain yield	Grain yield	A, B,C,M (S,P)***	5%	7.9	0.1
Forest trees (POD_1IAM)	Total biomass	Annual growth of living biomass of trees	A, B,C (S,P)	4%	5.7	0.6
			M	4%	13.7	1.7
(Semi-) natural vegetation (POD_1IAM)						
Temperate perennial grasslands	Flower number	Vitality of species-rich grasslands	A, B,C (S,P)	10%	6.6	0.1
Med. annual pastures	Flower/ seed biomass		M	10%	10.8	4.6

** A: Atlantic; B: Boreal; C: Continental, S: Steppic, P: Pannonian; M: Mediterranean. Suitable for vegetation types in regions not in brackets, but could also be applied to regions in brackets.*

*** Represents the (POD_ySPEC – Ref10 POD_ySPEC) required for a x% reduction*

**** Separate parameterisations should be used for Mediterranean and non-Mediterranean areas.*

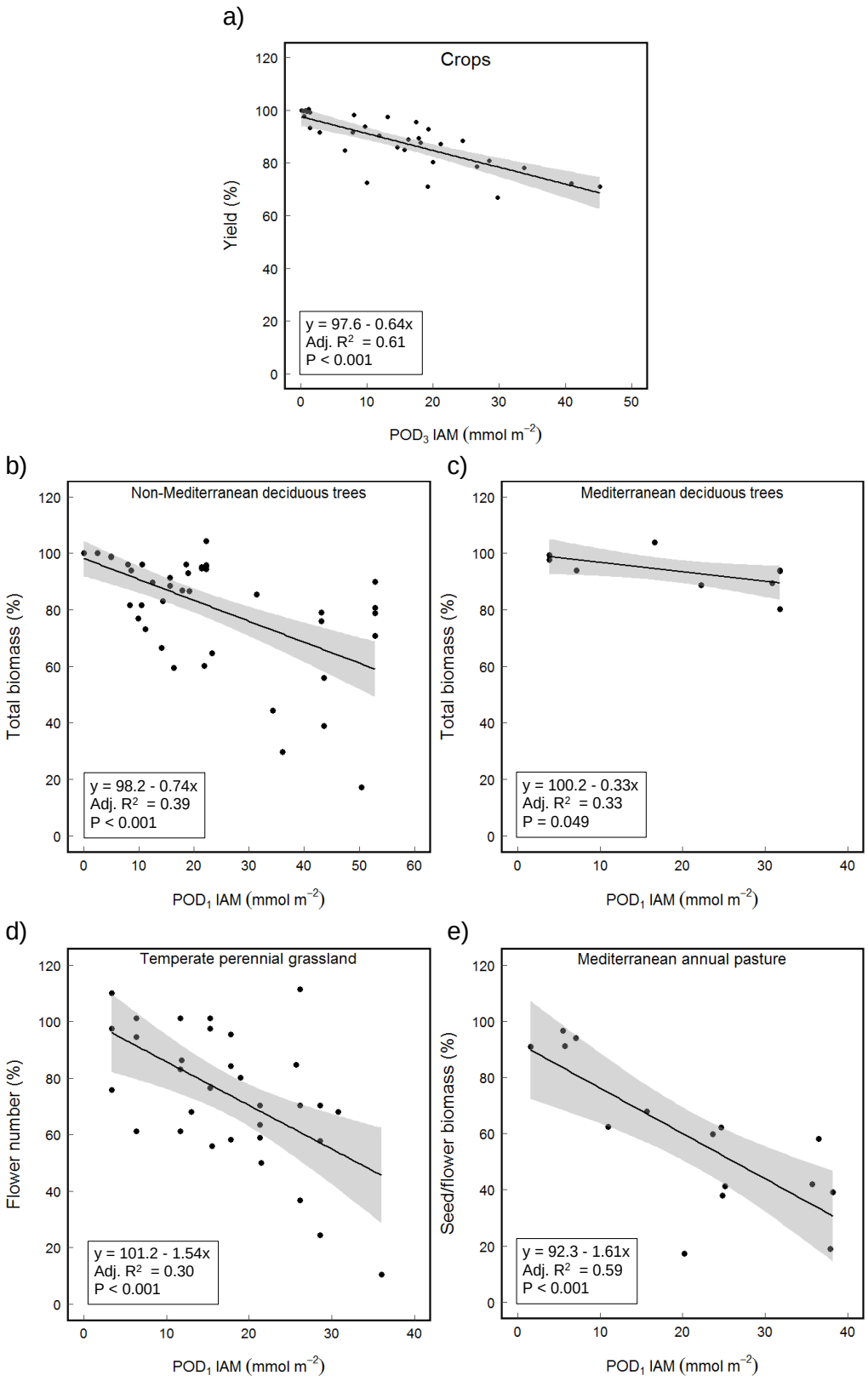

Figure III.15: *Flux (POD_YIAM) effect relationships for application in large-scale modelling, including Integrated Assessment Modelling (IAM), a) for crops, for broadleaf deciduous trees in b) non-Mediterranean and c) Mediterranean regions and for (semi-)natural vegetation in d) non-Mediterranean and e) Mediterranean regions.*

III.3.7 CONCENTRATION-BASED CRITICAL LEVELS FOR O_3 (AOT40)

III.3.7.1 APPLICATIONS

These are based on accumulation of the hourly mean O_3 concentration at the top of the canopy over a threshold concentration of 40 ppb during daylight hours (when global radiation is more than 50 W m^{-2}) for the appropriate time-window (AOT40) and thus do not take account of the stomatal influence on the amount of O_3 entering the plant. Hence, the spatial distribution of the risk of adverse impacts on vegetation generally mimics the spatial distribution of O_3 concentration and is different from the spatial distribution of POD_Y on the pan-European scale (Mills et al., 2011a, Simpson et al., 2007). Potential applications for AOT40-based critical levels are described in box 10.

Box 10: Applications for AOT40-based critical levels

AOT40-based critical levels are suitable for estimating the risk of damage where climatic data or suitable flux models are not available and/or areas where no climatic or water restrictions to stomatal O_3 flux are expected. Critical levels are defined for agricultural and horticultural crops, forests and (semi-)natural vegetation.

III.3.7.2 AOT40 METHODOLOGY FOR ALL VEGETATION TYPES

It is recommended that AOT40 values for comparison with the critical levels should be calculated as the mean value over the most recent five years for which appropriate quality assured data are available. For local and national risk assessment, it may also be valuable to choose the year with the highest AOT40 from the five years.

In summary, the following steps are required for calculation of AOT40 and exceedance of the critical level for a given year for a specific species/vegetation type:

Step 1: The vegetation- or species-specific accumulation period is determined.

Step 2: Collate the hourly mean O_3 concentrations for the measurement height and accumulation period.

Step 3: Adjust the O_3 data from measurement height to canopy height using an appropriate model or the algorithm in this manual (see Section III.3.4.2 and SBD-A).

Step 4: Calculate the AOT40 index by subtracting 40 from each hourly mean during daylight hours (when global radiation is more than 50 W m^{-2}) and then summing the resulting values (see example in Figure III.16).

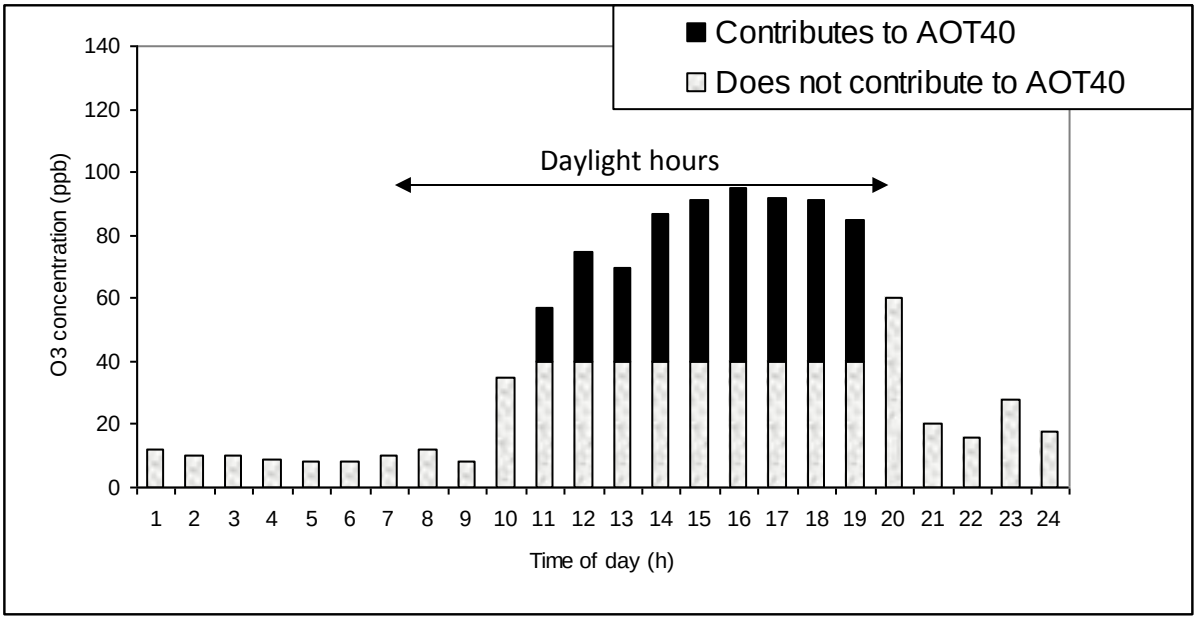

Figure III.16: Calculation of O_3 accumulated over a threshold of 40 ppb (AOT40) in ppb h for Balingen (6 May, 1992). The AOT40 for this day is 383 ppb h, calculated as 17 (exceedance of 40 ppb for 11th hour) + 35 (12th hour) + 30 (13th hour) + 47 (14th hour) + 51 (15th hour) + 55 (16th hour) + 52 (17th hour) + 51 (18th hour) + 45 (19th hour). Exceedance of 40 ppb in the 20th hour is not included because it occurred after daylight (global radiation was less than 50 W m^{-2}) had ended.

III.3.7.3 AOT40-BASED CRITICAL LEVELS FOR CROPS, FOREST TREES AND (SEMI-)NATURAL VEGETATION

Here we provide a summary of AOT40-based critical levels for vegetation, for further details see SBD-A.

Crops

AOT40-based critical levels have been defined for agricultural and horticultural crops, based on dose-response relationships for wheat (Mills et al., 2007) and tomato (González-Fernández et al., 2014) respectively (Table III.17). The timing of the three month accumulation period for agricultural crops should reflect the period of active growth of wheat and be centred on the timing of mid-anthesis (see Section III.3.5.2.1). For horticultural crops, the timing of the start of the growing season is more difficult to define because they are repeatedly sown over several months in many regions, especially in the Mediterranean. For local application within the Mediterranean, appropriate 3 month periods should be selected between March and August for eastern Mediterranean areas, and March and October for western Mediterranean areas. Since the cultivars used to derive the response function for tomato also grow in other parts of Europe, it is suggested that appropriate 3 month periods are selected between the period April to September for elsewhere in Europe.

Forest trees

AOT40-based critical levels have been defined for forest trees, based on dose-response relationships for beech and birch (Table III.17; Karlsson et al., 2003; 2007). The default window for the accumulation of AOT40 is 1 April to 30 September for all deciduous and evergreen species in Europe. This time period does not take altitudinal variation into account and should be viewed as indicative only. The default window should only be used where local information on the growing season, with start and end of the growing season clearly defined from measurements, the latitude model or phenological models, is not available.

(Semi-)natural vegetation

AOT40-based critical levels for (semi-)natural vegetation are applicable to all (semi-)natural vegetation. Two AOT40-based critical levels have been defined based on a limited number of sensitive species: one for communities dominated by annual, and one for communities dominated by perennial species (Table III.17).

Table III.17: *Summary of AOT40-based critical levels for vegetation.*

Vegetation type	Effect (% reduction at critical level)	Critical level (ppm h)	Accumulation period	Reference
Crops				
Agricultural	Grain yield (5%; based on wheat)	3	3 months	Mills et al, 2007
Horticultural	Fruit yield (5%; based on tomato)	8	3 months	González-Fernández et al., 2014
Trees				
	Total biomass (5%; based on beech and birch)	5	Growing season (default: 6 months)	Karlsson et al., 2003, 2007
(Semi-)natural vegetation				
Dominated by annuals	Above ground biomass (10%)	3	3 months (or growing season, if shorter)	Ashmore & Davidson, 1996; Fuhrer et al., 2003
Dominated by perennials	Effects on total above-ground or below-ground biomass and/or on the cover of individual species and/or on accelerated senescence of dominant species (10%)	5	6 months	UNECE, 2006

III.4 REFERENCES

Ainsworth, E. A., 2016. Understanding and improving global crop response to ozone pollution. The Plant Journal. doi: 10.1111/tpj.13298.

Ainsworth, E.A., Yendrek, C.R., Sitch, S., Collins, W.J., Emberson, L.D., 2012. The effects of tropospheric ozone on net primary productivity and implications for climate change. Annual Review of Plant Biology 63, 637-661.

Aranda, I., Gil L., Pardos, J.A., 2005. Seasonal changes in apparent hydraulic conductance and their implications for water use of European beech (*Fagus sylvatica* L.) and sessile oak [*Quercus petraea* (Matt. Liebl)] in South Europe. Plant Ecology 179, 155-167.

Ashmore, M.R., Davison, A.W., 1996. Towards a critical level of ozone for natural vegetation. In: Kärenlampi, L. & Skärby, L., (Eds.). Critical levels for ozone in Europe: testing and finalising the concepts. UNECE Workshop Report. University of Kuopio, Department of Ecology and Environmental Science, pp. 58-71.

Ashmore, M.R., Wilson, R.B. (Eds.), 1993. Critical levels of Air Pollutants for Europe. Background Papers prepared for the ECE Workshop on critical levels, Egham, UK, 23-26 March 1992.

Bassin, S., Kach, D., Valsangiacomo, A., Mayer, J., Oberholzer, H.-R., Volk, M., Fuhrer, J., 2015. Elevated ozone and nitrogen deposition affect nitrogen pools of subalpine grassland. Environmental Pollution 201, 67-74.

Bassin, S., Volk, M., Fuhrer, J., 2007. Factors affecting the ozone sensitivity of temperate European grasslands: An overview. Environmental Pollution 146, 678-691.

Bassin, S., Volk, M., Fuhrer, J., 2013. Species composition of subalpine grassland is sensitive to nitrogen deposition, but not to ozone, after seven years of treatment. Ecosystems 16, 1105-1117.

Battilani, A., Prieto, H., Argerich, C., Campillo, C., Cantore, V., 2012. Tomato. In: Steduto, P., Hsiao, T., Fereres, E., Raes D. (Eds.) Crop yield response to water. FAO irrigation and drainage paper 66. Food and Agriculture Organization of the United Nations, Rome, pp 192-198.

Bergmann, E., Bender, J., Weigel, H.-J., 2015. Assessment of the impacts of ozone on biodiversity in terrestrial ecosystems: Literature review and analysis of methods and uncertainties in current risk assessment approaches. Part II: Literature review of the current state of knowledge on the impact of ozone on biodiversity in terrestrial ecosystems. Umwelt Bundesamt TEXTE 71/2015, Dessau-Roßlau, Germany. ISSN 1862-4804.

Braun, S., Schindler, C., Rihm, B., 2014. Growth losses in Swiss forests caused by ozone: Epidemiological data analysis of stem increment of *Fagus sylvatica* L. and *Pica abies* Karst. Environmental Pollution 192, 129-138.

Büker, P., Feng, Z., Uddling, J., Briolat, A., Alonso, R., Braun, S., Elvira, S., Gerosa, G., Karlsson, P.E., Le Thiec, D., Marzuoli, R., Mills, G., Oksanen, E., Wieser, G., Wilkinson, M., Emberson, L.D., 2015. New flux based dose–response relationships for ozone for European forest tree species. Environmental Pollution 206:163–174.

Büker, P., Morrissey, T., Briolat, A., Falk, R., Simpson, D., Tuovinen, J.-P., Alonso, R., Barth, S., Baumgarten, M., Grulke, N., Karlsson, P.E., King, J., Lagergren, F., Matyssek, R., Nunn, A., Ogaya, R., Peñuelas, J., Rhea, L., Schaub, M., Uddling, J., Werner, W., Emberson, L.D., 2012. DO_3SE modelling of soil moisture to determine ozone flux to forest trees. Atmospheric Chemistry and Physics 12, 5537–5562.

Calatayud, V., Cerveró, J., Calvo, E., García-Breijo, F.J., Reig-Armiñana, J., Sanz, M.J., 2011. Responses of evergreen and deciduous Quercus species to enhanced levels. Environmental Pollution 159, 55-63.

Campbell, G.S., Norman, J.M., 2000. An introduction to environmental biosphysics (2nd edition). Springer, USA, pp. 286.

Damesin, C., Rambal, S., 1995. Field study of leaf photosynthetic performance by a Mediterranean deciduous oak tree (*Quercus pubescens*) during a severe summer drought. New Phytologist 131, 159-167.

Danielsson, H., Pihl Karlsson, G., Karlsson, P. E., Pleijel, H., 2003. Ozone uptake modelling and flux-response relationships – assessments of ozone-induced yield loss in spring wheat. Atmospheric Environment 37, 475-485.

Di Gegorio, A., Jansen, L.J.M., 2000. Land cover classification system (LCCS): Classification concept and user manual. FAO, Rome, Italy.

Duchemin, B., Goubier, J., Courrier, G., 1999. Monitoring phenological key stages and cycle duration of temperate deciduous forest ecosystems with NOAA/AVHRR data. Remote Sensing of Environment 67, 68-82.

EEA, 2016. Biogeographical regions in Europe. http://www.eea.europa.eu/data-and-maps/data/biogeographical-regions-europe-3

Emberson, L.D., Ashmore, M.R., Cambridge, H.M., Simpson, D., Tuovinen, J.-P., 2000a. Modelling stomatal ozone flux across Europe. Environmental Pollution 109, 403-413.

Emberson, L.D., Ashmore, M.R., Simpson, D., Tuovinen, J.-P., Cambridge, H.M., 2001. Modelling and mapping ozone deposition in Europe. Water, Air and Soil Pollution 130, 577–582.

Emberson, L.D., Büker, P., Ashmore, M.R., 2007. Assessing the risk caused by ground level ozone to European forest trees: A case study in pine, beech and oak across different climate regions. Environmental Pollution 147, 454–466.

Emberson, L. D., Büker, P, Ashmore, M.R., Mills, G., Jackson, L.S., Agrawal, M., Atikuzzaman, M.D., Cinderby, S., Enghardt, M., Jamir, C., Kobayashi, K., Oanh, T.T.K., Quadir, Q.F., Wahid, A., 2009. A comparison of North American and Asian exposure–response data for ozone effects on crop yields. Atmospheric Environment 43, 1945-1953.

Emberson, L.D., Wieser, G., Ashmore, M.R., 2000b. Modelling of stomatal conductance and ozone flux of Norway spruce: comparison with field data. Environmental Pollution 109, 393–402.

Feng, Z., Hu, E., Wang, X., Jiang, L., Liu, X., 2015. Ground-level O3 pollution and its impacts on food crops in China: A review. Environmental Pollution 199, 42-48.

Frati L., Santoni S., Nicolardi V., Gaggi C., Brunialti G., Guttova A., Gaudino S., Pati A., Pirintsos S.A., Loppi S., 2007. Lichen biomonitoring of ammonia emission and nitrogen deposition around a pig stockfarm. Environmental Pollution 146, 311-316.

Fuhrer, J., 1994. The critical level for ozone to protect agricultural crops – An assessment of data from European open-top chamber experiments. In: Fuhrer J. & Achermann, B., (Eds). Critical Levels for Ozone. UNECE Workshop Report, Schriftenreihe der FAC Berne-Liebefeld, pp. 42-57.

Fuhrer, J., Ashmore, M.R., Mills, G., Hayes, F., Davison, A.W., 2003. Critical levels for semi-natural vegetation. In: Karlsson, P.E., Selldén, G. & Pleijel, H., (Eds). Establishing Ozone Critical Levels II. UNECE Workshop Report. IVL report B 1523. IVL Swedish Environmental Research Institute, Gothenburg, Sweden, pp. 183-198.

Fuhrer, J., Martin, M.V., Mills, G., Heald, C.L., Harmens, H., Hayes, F., Sharps, K., Bender, J., Ashmore, M.R., 2016. Current and future ozone risks to global terrestrial biodiversity and ecosystem processes. Ecology & Evolution 6, 8785-8799.

Gerosa, G., Finco, A., Marzuoli, R., Ferretti, M., Gottardini, E., 2012. Errors in ozone risk assessment using standard conditions for converting ozone concentrations obtained by passive samplers in mountain regions. Journal of Environmental Monitoring 14, 1703-1709.

Gimeno B. S., Bermejo V., Sanz J., De La Torre D., Elvira S., 2004a. Growth response to ozone of annual species from Mediterranean pastures. Environmental Pollution, 132, 297–306.

Gimeno, B.S. Bermejo, V., Sanz, J., De la Torre, D., Gil, J.M., 2004b. Assessment of the effects of ozone exposure and plant competition on the reproductive ability of three therophytic clover species from Iberian pastures. Atmospheric Environment 38, 2295 – 2303.

González-Fernández, I., Bermejo, V., Elvira, S., de la Torre, D., González, A., Navarrete, L., Sanz, J., Calvete, H., Garcia-Gomez, H., Lopez, A., Serra, J., Lafarga, A., Armesto, A.P., Calvo, A., Alonso, R., 2013. Modelling ozone stomatal flux of wheat under mediterranean conditions. Atmospheric Environment 67, 149-160.

González-Fernández, I., Calvo, E., Gerosa, G., Bermejo, V., Marzuoli, R., Calatayud, V., Alonso, R., 2014. Setting ozone critical levels for protecting horticultural Mediterranean crops: Case study of tomato. Environmental Pollution 185, 178-187.

Gottardini, E., Calatayud, V., Ferretti, M., Haeni, M., Schaub, M., 2016. Spatial and temporal distribution of ozone symptoms across Europe from 2002 to 2014. In: Michel, A., Seidling, W. (Eds.). Forest condition in Europe: 2016 technical report of ICP Forests. BFW-Dokumentation 23/2016. Vienna: BFW Austrian Research Centre for Forests, pp. 73-82.

Grassi, G., Magnani, F., 2005. Stomatal, mesophyll conductance and biochemical limitations to photosynthesis as affected by drought and leaf ontogeny in ash and oak trees. Plant, Cell and Environment 28, 834-849.

Grünhage, L., Pleijel, H., Mills, G., Bender, J., Danielsson, H., Lehmann, Y., Castell, J.-F., Bethenod, O., 2012. Updated stomatal flux and flux-effect models for wheat for quantifying effects of ozone on grain yield, grain mass and protein yield. Environmental Pollution 165, 147-157.

Harmens, H., G. Mills (Eds.), 2012. Ozone pollution: Impacts on carbon sequestration in Europe. Centre for Ecology & Hydrogogy, Bangor, UK. ISBN: 978-1-906698-31-7.

Hayes, F., Jones, M.L.M., Mills, G. & Ashmore, M., 2007. Meta-analysis of the relative sensitivity of semi-natural vegetation species to ozone. Environmental Pollution 146, 754-762.

Hayes, F., Mills, G., Harmens, H., Wyness, K., 2011. Within season and carry-over effects following exposure of grassland species mixtures to increasing background ozone. Environmental Pollution 159, 2420-2426.

Hayes, F., Wagg, S., Mills, G., Wilkinson, S., Davies, W., 2012. Ozone effects in a drier climate: implications for stomatal fluxes of reduced stomatal sensitivity to soil drying in a typical grassland species. Global Change Biology 18, 948-959.

Hewitt, D.K.L., Mills, G., Hayes, F., Wilkinson, S., Davies, W., 2014. Highlighting the threat from current and near-future ozone pollution to clover in pasture. Environmental Pollution 189, 111-117.

Jarvis, P.G., 1976. The interpretation of the variations in leaf water potential and stomatal conductance found in canopies in the field, Philos. Trans. R. Soc. Lond., B 273, 593-610.

Karlsson, P.E., Uddling, J., Braun, S., Broadmeadow, M., Elvira, S., Gimeno, B.S., Le Thiec, D., Oksanen, E., Vandermeiren, K., Wilkinson, M., Emberson, L., 2003. new critical levels for ozone impact on

trees based on AOT40 and leaf cumulated uptake of ozone. In: Karlsson, P.E., Selldén, G., Pleijel, H., (Eds.). Establishing Ozone Critical Levels II. UNECE Workshop Report. IVL report B 1523.

Karlsson, P.E., Braun, S., Broadmeadow, M., Elvira, S., Emberson, L., Gimeno, B.S., Le Thiec, D., Novak, K., Oksanen, E., Schaub, M., Uddling, J. Wilkinson, M., 2007. Risk assessments for forest trees - the performance of the ozone flux versus the AOT concepts. Environmental Pollution 146, 608-616.

Leith I.D., van Dijk N., Pitcairn C.E.R., Wolseley P.A., Whitfield C.P., Sutton M.A., 2005. Biomonitoring methods for assessing the impacts of nitrogen pollution: refinement and testing, JNCC Report No. 386, JNCC, Peterborough, pp. 290.

Matyssek, R., Wieser, G., Calfapietra, C., De Vries, W., Dizengremel, P., Ernst, D., Jolivet, Y., Mikkelsen, T.N., Mohren, G.M.J., Le Thiec, D., Tuovinen, J.-P., Weatherall, A., Paoletti, E., 2012. Forests under climate change and air pollution: Gaps in understanding and future directions for research. Environmental Pollution, 160, 57-65.

Marzuoli, R., Monga, R., Finco, A., Gerosa, G., 2016. Biomass and physiological responses of *Quercus robur* (L.) young trees during 2 years of treatments with different levels of ozone and nitrogen wet deposition. Trees 30, 1995-2010.

Massman, W.J., 1998. A review of the molecular diffusivities of H_2O, CO_2, CH_4, CO, O_3, SO_2, NH_3, N_2O, NO, and NO_2 in air, O_2 and N_2 near STP. Atmospheric Environment 32, 1111-1127.

McNaughton, K.G., Van der Hurk, B.J.J.M., 1995. 'Lagrangian' revision of the resistors in the two-layer model for calculating the energy budget of a plant canopy. Boundary Layer Meteorology 74, 261-288.

Mediavilla, S., Escudero, A.E., 2003. Stomatal responses to drought at a Mediterranean site: a comparative study of co-occurring woody species differing in leaf longevity. Tree Physiology 23, 987–996.

Mills, G.E**.**, Ball, G.R., 1998. Annual Progress Report for the ICP-Crops (September 1997-August 1998). Centre for Ecology & Hydrology, Bangor, UK.

Mills, G., Buse, A., Gimeno, B., Bemejo, V., Holland, M., Emberson, L. & Plejel, H., 2007. A synthesis of AOT40-based response functions and critical levels of ozone for agricultural and horticultural crops. Atmospheric Environment 41, 2630 – 2643.

Mills, G., Harmens, H. (Eds.), 2011. Ozone pollution: A hidden threat to food security. Centre for Ecology & Hydrogogy, Bangor, UK. ISBN: 978-1-906698-27-0.

Mills, G., Hayes, F., Simpson, D., Emberson, L., Norris, D., Harmens, H., Büker, P., 2011a. Evidence of widespread effects of ozone on crops and (semi-)natural vegetation in Europe (1990–2006) in relation to AOT40- and flux-based risk maps. Global Change Biology 17, 592-613.

Mills, G., Pleijel, H., Braun, S., Büker, P., Bermejo, V., Calvo, E., Danielsson, H., Emberson, L., Fernandez, I.G., Grunhage, L., Harmens, H., Hayes, F., Karlsson, P.E., Simpson, D., 2011b. New stomatal flux-based critical levels for ozone effects on vegetation. Atmospheric Environment 45, 5064-5068.

Mills, G., Wagg, S., Harmens, H. (Eds.), 2013. Ozone Pollution: Impacts on ecosystem services and biodiversity. Centre for Ecology & Hydrogogy, Bangor, UK. ISBN No. 978-1-906698-39-3.

Payne, R. J., Stevens, C. J. Dise, N.B., Gowing, D.J., Pilkington, M.G., Phoenix, G.K., Emmett, B.A., Ashmore, M.R., 2011. Impacts of atmospheric pollution on the plant communities of British acid grasslands. Environmental Pollution 159, 2602-2608.

Peterson, R.F., 1965. Wheat: Botany, cultivation, and utilization. Leonard Hill Books, London.

Pinho P., Branquinho C., Cruz C., Tang S.Y., Dias T., Rosa A.P., Máguas C., Louçãoa M.A.M., Sutton M.A., 2009. Assessment of critical levels of atmospherically ammonia for lichen diversity in cork-oak

woodland, Portugal. In: Sutton M.A., Baker S., Reis S., (Eds.), Atmospheric Ammonia - Detecting emission changes and environmental impacts. Springer, Berlin, 109-119.

Pitcairn C.E.R., Leith I.D., Sheppard L.J., van Dijk N., Tang Y.S., Wolseley P.A., James P., Sutton M.A., 2004. Field intercomparison of different bio-indicator methods to assess the effects of atmospheric nitrogen deposition, in: Sutton M.A., Pitcairn C.E.R., Whitfield C.P. (Ed.), Bioindicator and biomonitoring methods for assessing the effects of atmospheric nitorgen on statutory nature conservation sites, JNCC Report 356, pp. 168-177.

Pleijel, H., 2011. Reduced ozone by air filtration consistently improved grain yield in wheat. Environmental Pollution 159, 897-902.

Pleijel, H., Danielsson, H., Emberson, L., Ashmore, M., Mills, G., 2007. Ozone risk assessment for agricultural crops in Europe: Further development of stomatal flux and flux–response relationships for European wheat and potato. Atmospheric Environment 4, 3022-3040.

Pleijel, H., Danielsson, H., Vandermeiren, K., Blum, C., Colls, J., Ojanperä, K., 2002. Stomatal conductance and ozone exposure in relation to potato tuber yield – results from the European CHIP programme. European Journal of Agronomy 17, 303-317.

Rihm B., Urech M., Peter K., 2009. Mapping ammonia emissions and concentrations for Switzerland – Effects on lichen vegetation. In: Sutton M.A., Baker S., Reis S., (Eds.), Atmospheric Ammonia - Detecting emission changes and environmental impacts. Springer, Berlin, pp. 87-92.

Sanz, J., Bermejo, V., Gimeno, B.S., Elvira, S., Alonso, R. 2007. Ozone sensitivity of the Mediterranean terophyte *Trifolium striatum* is modulated by soil nitrogen content. Atmospheric Environment 41, 8952–8962.

Sanz, J., González-Fernández, I., Calvete-Sogo, H., Lin, J.S., Alonso, R., Muntifering, R., Bermejo, V., 2014. Ozone and nitrogen effects on yield and nutritive quality of the annual legume *Trifolium cherleri*. Atmospheric Environment 94,765–772.

Sanz, J., González-Fernández, I., Elvira, S., Muntifering, R., Alonso, R., Bermejo-Bermejo, V., 2016. Setting ozone critical levels for annual Mediterranean pasture species : Combined analysis of open-top chamber experiments. Science of the Total Environment 571, 670-679.

Sanz, J., Muntifering, R.B., Gimeno, B.S., Bermejo, V., Elvira, S., 2005. Ozone and increased nitrogen supply effects on the yield and nutritive quality of *Trifolium subterraneum*. Atmospheric Environment 39, 5899–5907.

Sheppard L.J., Leith I.D., Crossley A., van Dijk N., Fowler D., Sutton M.A., 2009. Long-term cumulative exposure exacerbates the effects of atmospheric ammonia on an ombrotrophic bog: Implications for Critical Levels. In: Sutton M.A., Baker S., Reis S., (Eds.), Atmospheric Ammonia - Detecting emission changes and environmental impacts. Springer, Berlin, 49-58.

Simpson, D., Ashmore, M.R., Emberson, L., Tuovinen, J.P., 2007. A comparison of two different approaches for mapping potential ozone damage to vegetation. A model study. Environmental Pollution 146, 715-725.

Simpson, D., Benedictow, A., Berge, H., Bergström, R., Emberson, L.D., Fagerli, H., Flechard, C.R., Hayman, G.D., Gauss, M., Jonson, J.E., Jenkin, M.E., Nýıri, A., Richter, C., Semeena, V.S., Tsyro, S., Tuovinen, J.-P., Valdebenito, Á., Wind, P., 2012. The EMEP MSC-W chemical transport model – technical description. Atmospheric Chemistry and Physics 12, 7825-7865.

Sutton M.A., Wolseley P.A., Leith I.D., van Dijk N., Tang Y.S., James P.W., Theobald M.R., Whitfield C.P., 2009. Estimation of the ammonia critical level for epiphytic lichens based on observations at farm, landscape and national scales. In: Sutton M.A., Baker S., Reis S., (Eds.), Atmospheric Ammonia - Detecting emission changes and environmental impacts. Springer, Berlin, pp. 71-86.

Temple, P.J., Bytnerowicz, A.J., Fenn, M.E., Poth, M.A., 2005. Air pollution impacts in the mixed conifer forests of Southern California. In: Kus, B.E., Beyers, J.L. (Eds.). Planning for biodiversity: Bringing research and management together. USDA Forest Service Gen. Tech. Rep. PSW-GTR-195.

Uddling, J., Pleijel, H., Karlsson, P.E., 2004. Modelling leaf diffusive conductance in juvenile silver birch, *Betula pendula*. Trees 18, 686-695.

UNECE, 2006. Report on the workshop on critical levels of ozone: further applying and developing the flux-based concept. ECE/EB.AIR/WG.1/2006/11.

UNECE, 2007. Report of workshop on atmospheric ammonia:detecting emission changes and environmental impacts. ECE/EB.AIR/WG.5/2007/3.

UNECE, 1996. Manual on methodologies and criteria for mapping critical levels/loads and geographical areas where they are exceeded. Texte 71/96, Umweltbundesamt, Berlin, Germany.

U.S. Environmental Protection Agency, 2014. Welfare risk and exposure assessment for ozone. EPA-452/R-14-005a, North Carolina, USA, pp. 7.1-7.65.

Volk, M., Wolff, V., Bassin, S., Ammann, C., Fuhrer, J., 2014. High tolerance of subalpine grassland to long-term ozone exposure is independent of N input and climatic drivers, Environmental Pollution 189, 161–168.

Wagg, S., Mills, G., Hayes, F., Wilkinson, S., Cooper, D., Davies, W.J., 2012. Reduced soil water availability did not protect two competing grassland species from the negative effects of increasing background ozone. Environmental Pollution 165, 91-99.

WHO, 2000. Air Quality Guidelines for Europe. WHO Regional Publications, No. 91, World Health Organisation, Copenhagen. http://www.euro.who.int/en/publications

Wittig, V.E., Ainsworth, E.A., Naidu, S.L., Karnosky, D.F., Long, S.P., 2009. Quantifying the impact of current and future tropospheric ozone on tree biomass, growth, physiology and biochemistry: a quantitative meta-analysis.Global Change Biology 15, 396-424.

Wolseley P.A., James P.W., Theobald M.R., Sutton M.A., 2006. Detecting changes in epiphytic lichen communities at sites affected by atmospheric ammonia from agricultural sources. Lichenologist 38, 161-176.

Wyness, K., Mills, G., Jones, L., Barnes, J.D., Jones, D.L., 2011. Enhanced nitrogen deposition exacerbates the negative effect of increasing background ozone in *Dactylis glomerata*, but not *Ranunculus acris*. Environmental Pollution 159, 2493-2499.

Zhang, X., Friedl, M.A, Schaaf, C.B., Strahler, A.H., 2004. Climate controls on vegetation phenological patterns in northern mid- and high latitudes inferred from MODIS data. Global Change Biology 10, 1133-1145.

III.5 ANNEXES FOR CHAPTER 3

III.5.1 ANNEX 1: HISTORY OF THE DEVELOPMENT OF THE INCLUDED CRITICAL LEVELS

The critical level values have been set, reviewed and revised for O_3, SO_2, NO_x and NH_3 at a series of UNECE Workshops and associated Task Force meeting of the ICP Vegetation:

- Bad Harzburg (1988; UNECE, 1988);
- Bad Harzburg (1989);
- Egham (1992; Ashmore & Wilson, 1993);
- Bern (1993; Fuhrer & Achermann, 1994);
- Kuopio (1996; Kärenlampi & Skärby, 1996);
- Gerzensee (1999; Fuhrer & Achermann, 1999);
- Gothenburg (2002; Karlsson et al., 2003);
- Obergurgl (2005; Wieser & Tausz, 2006);
- Edinburgh (2006; UNECE, 2007; Sutton et al., 2009);
- Ispra (2009);
- Tervuren (23rd ICP Vegetation Task Force Meeting, 2010, UNECE 2010; Mills et al., 2011)
- Madrid (2016); preceded by preparatory meetings in Hindås (2015) and Deganwy (2016).
- Poznan (30th ICP Vegetation Task Force Meeting, 2017; UNECE, 2017)

The earliest version of this manual (UNECE, 1996) included concentration-based critical levels that used AOTX (O_3 concentrations accumulated over a threshold of X ppb) as the O_3 parameter. However, several important limitations and uncertainties have been recognised for using AOTX. In particular, the real impacts of O_3 depend on the amount of O_3 reaching the sites of damage within the leaf, whereas AOT40-based critical levels only consider the O_3 concentration at the top of the canopy.

The Gerzensee Workshop in 1999 recognised the importance of developing an alternative approach based on the flux of O_3 from the exterior of the leaf through the stomatal pores to the sites of damage (stomatal flux or Phytotoxic Ozone Dose above a threshold flux of Y nmol m^{-2} PLA s^{-1}; POD_Y). This approach required the development of mathematical models to estimate stomatal flux, primarily from knowledge of stomatal responses to environmental factors. It was agreed at the Gothenburg Workshop in 2002 that O_3 flux-effect models were sufficiently robust for the derivation of flux-based critical levels, and such critical levels should be included in this chapter for wheat, potato and provisionally for beech and birch combined. An additional simplified flux-based "worst-case" risk assessment method for use in large-scale and integrated assessment modelling was discussed at the Obergurgl Workshop (2005) and after further revision (approved at appropriate Task Force meetings) is included here.

At the Hindås meeting (2015), Deganwy meeting (2016), Madrid Workshop (2016) and subsequent 30th Task Force meeting of the ICP Vegetation (2017) in Poznan, the methodology, flux-effect relationships and critical levels were reviewed and revised where needed, and added for new (groups of) species or vegetation types. The current version of this chapter incorporates all of these new/revised flux-based critical levels together with the updated AOT40-based critical levels (no changed made). Currently, 16 species or groups of species-specific vs (based on POD_YSPEC) and 5 vegetation type-specific critical levels (based on POD_YIAM) are included.

The critical levels and risk assessment methods for vegetation described in this chapter were prepared by leading European experts from available knowledge on impacts gaseous air pollutants on vegetation, and thus represent the current "state of knowledge".

References

Ashmore, M.R., Wilson, R.B. (Eds.), 1993. Critical levels of Air Pollutants for Europe. Background Papers prepared for the ECE Workshop on critical levels, Egham, UK, 23-26 March 1992.

Fuhrer, J., Achermann, B. (Eds,), 1994. Critical Levels for Ozone. UNECE Workshop Report, Schriftenreihe der FAC Berne-Liebefeld.

Fuhrer, J., Achermann, B. (Eds), 1999. Critical Levels for Ozone – Level II. Swiss Agency for the Environment, Forests and Landscape, Berne. Environmental Documentation No. 115.

Kärenlampi, L., Skärby, L. (Eds), (1996. Critical levels for ozone in Europe: testing and finalising the concepts. UNECE Workshop Report. University of Kuopio, Department of Ecology and Environmental Science.

Karlsson, P.E., Selldén, G., Pleijel, H. (Eds), 2003. Establishing Ozone Critical Levels II. UNECE Workshop Report. IVL report B 1523. IVL Swedish Environmental Research Institute, Gothenburg, Sweden.

Mills, G., Pleijel, H., Braun, S., Büker, P., Bermejo, V., Calvo, E., Danielsson, H., Emberson, L., Fernandez, I.G., Grunhage, L., Harmens, H., Hayes, F., Karlsson, P.E., Simpson, D., 2011. New stomatal flux-based critical levels for ozone effects on vegetation. Atmospheric Environment 45, 5064-5068.

Sutton, M.A., Reis, S., Baker, S.M.H., 2009. Atmospheric ammonia - Detecting emission changes and environmental impacts. Springer Verlag, Berlin.

UNECE, 1988. Final Draft Report of the Critical Levels Workshop, Bad Harzburg, Germany, 14-18 March 1988.

UNECE, 2007. Report of workshop on atmospheric ammonia:detecting emission changes and environmental impacts. ECE/EB.AIR/WG.5/2007/3.

UNECE, 2010. Flux-based assessment of ozone effects for air pollution policy. Technical report from the ozone workshop in Ispra, 9 – 12 November, 2009. ECE/EB.AIR/WG.1/2010/13.

UNECE, 2017. Effects of air pollution on natural vegetation and crops. Technical report from the Programme Coordinating Centre of the ICP Vegetation. ECE/EB.AIR/GE.1/2016/14 - ECE/EB.AIR/WG.1/2016/7.

Wieser, G., Tausz, M. (Eds), 2006. Proceedings of the workshop: Critical levels of ozone: further applying and developing the flux-based concept, Obergurgl, November, 2005.

III.5.2 ANNEX 2: TERMINOLOGY

Table A.1: *Terminology for calculating O_3 critical levels for vegetation.*

Term	Abbreviation [Units]	Explanation
Terminology for flux-based critical levels		
Projected leaf area	PLA [m^2]	The projected leaf area is the total area of the sides of the leaves that are projected towards the sun. PLA is in contrast to the total leaf area, which considers both sides of the leaves. For horizontal leaves the total leaf area is simply 2*PLA.
Stomatal flux of O_3	F_{st} [nmol m^{-2} PLA s^{-1}]	Instantaneous flux of O_3 through the stomatal pores per unit projected leaf area (PLA). F_{st} can be defined for any part of the plant, or the whole leaf area of the plant, but for this manual, F_{st} refers specifically to the sunlit leaves at the top of the canopy. F_{st} is normally calculated from hourly mean values and is regarded here as the hourly mean flux of O_3 into the stomata.
Stomatal flux of O_3 above a flux threshold of Y nmol m^{-2} PLA s^{-1}	$F_{st}Y$ [nmol m^{-2} PLA s^{-1}]	Instantaneous flux of O_3 above a flux threshold of Y nmol m^{-2} PLA s^{-1}, through the stomatal pores per unit projected leaf area. $F_{st}Y$ can be defined for any part of the plant, or the whole leaf area of the plant, but for this manual $F_{st}Y$ refers specifically to the sunlit leaves at the top of the canopy. $F_{st}Y$ is normally calculated from hourly mean values and is regarded here as the hourly mean flux of O_3 through the stomata.
Phytotoxic O_3 dose above a flux threshold of Y nmol m^{-2} PLA s^{-1}	POD_Y [mmol m^{-2} PLA]	Phytotoxic O_3 dose (POD) is the accumulated flux above a flux threshold of Y nmol m^{-2} PLA s^{-1}, accumulated over a stated time period during daylight hours. Similar in mathematical concept to AOT40.
Phytotoxic O_3 dose calculated for a specific plant species or group of plant species	POD_YSPEC [mmol m^{-2} PLA]	Phytotoxic O_3 dose above a flux threshold of Y nmol m^{-2} PLA s^{-1} for a specific plant species or group of plant species (POD_YSPEC), accumulated over a stated time period during daylight hours.
Phytotoxic O_3 dose calculated for a for a vegetation type	POD_YIAM [mmol m^{-2} PLA]	Phytotoxic O_3 dose above a flux threshold of Y nmol m^{-2} PLA s^{-1} for a vegetation type for application in large-scale modelling such as integrated assessment modelling (POD_YIAM), accumulated over a stated time period during daylight hours.
Reference POD_Y at constant 10 ppb O3, representing average 'pre-industrial' O_3 concentration	Ref10 POD_Y [mmol m^{-2} PLA]	Phytotoxic O_3 dose above a flux threshold of Y nmol m^{-2} PLA s^{-1} calculated at a constant O_3 concentration of 10 ppb, accumulated over a stated time period during daylight hours.
Flux-based critical level of O_3	Flux-based CL [mmol m^{-2} PLA]	Phytotoxic O_3 dose above a flux threshold of Y nmol m^{-2} PLA s^{-1} (POD_Y), over a stated time period during daylight hours, above which direct adverse effects may occur on sensitive vegetation according to present knowledge.
Terminology for concentration-based critical levels		
Concentration accumulated over a threshold O_3 concentration of 40 ppb	AOT40 [ppm h]	The sum of the differences between the hourly mean O_3 concentration (in ppb) and 40 ppb when the concentration exceeds 40 ppb during daylight hours[1)], accumulated over a stated time period. Units of ppb and ppm are parts per billion (nmol mol^{-1}) and parts per million (µmol mol^{-1}) respectively, calculated on a volume/volume basis.
Concentration-based critical level of O_3	Concentration -based CL [ppm h]	AOT40 over a stated time period, above which direct adverse effects on sensitive vegetation may occur according to present knowledge.

III.5.3 ANNEX 3: DATA SOURCES AND REFERENCES FOR FLUX-EFFECT RELATIONSHIPS

III.5.3.1 CROPS

Table A2 provides a summary of the data sources and O_3 flux-effect relationships for crops as described in Section III.3.5.2.

Table A2: *Date sources and response functions for agricultural crops.*

Crop	**Wheat**	**Wheat**	**Wheat**	**Potato**	**Tomato**	**Tomato**
Effect parameter	**Grain yield**	**1000 grain weight**	**Protein yield**	**Tuber yield**	**Fruit yield**	**Fruit quality**
% reduction for critical level	5%	5%	5%	5%	5%	5%
Critical level (POD_6SPEC, mmol m^{-2})	**1.3**	**1.5**	**2.0**	**3.8**	**2.0**	**3.8**
Biogeographical region*	A,B,C,M (S,P)	A,B,C,M (S,P)	A,B,C,M (S,P)	A,B,C (M,S,P)	M (A,B,C,S,P)	M (A,B,C,S,P)
Countries involved in experiments	Belgium, Finland, Italy, Sweden	Belgium, Finland, Sweden	Belgium, Finland, Sweden	Belgium, Finland, Germany, Sweden	Italy, Spain	Italy, Spain
Number of data points	36	33	33	17	17	17
Number of cultivars	5	4	4	1	5 (sensitive cultivars only)	5 (sensitive cultivars only)
Data sources	Pleijel et al., 2007	Piikki et al., 2008	Piikki et al., 2008	Pleijel et al., 2007	González-Fernández et al., 2014	González-Fernández et al., 2014
Time period	200 ^{0}C days before anthesis to 700 ^{0}C days after anthesis	200 ^{0}C days before anthesis to 700 ^{0}C days after anthesis	200 ^{0}C days before anthesis to 700 ^{0}C days after anthesis	1130 ^{0}C days starting at plant emergence	250 to 1500 ^{0}C days starting at planting in the field (at 4th true leaf stage)	250 to 1500 ^{0}C days starting at planting in the field (at 4th true leaf stage)
Response function	RY(%) = 100.3 - 3.85 x POD_6SPEC	RY(%) = 100.6 - 3.35 x POD_6SPEC	RY(%) = 101.1 - 2.54 x POD_6SPEC	RY(%) = 101.4 – 1.34 x POD_6SPEC	RY(%) = 99.3 - 2.53 x POD_6SPEC	RY(%) = 99.7 - 1.30 x POD_6SPEC
Adjusted R^2	0.83	0.71	0.61	0.80	0.61	0.55
P value	<0.001	<0.001	<0.001	<0.001	<0.001	<0.001
Data curator (E-mail)	Håkan Pleijel (hakan.pleijel@bioenv.gu.se)				Ignacio González-Fernández (ignacio.gonzalez@ciemat.es)	

** A = Atlantic; B = Boreal; C, = Continental, M = Mediterranean, S = Steppic, P = Pannonian. In brackets: not derived for those regions but could be applied there too.*

III.5.3.2 FOREST TREES

Table A3 provides a summary of the data sources and O_3 flux-effect relationships for forest trees as described in section III.3.5.3.

Table A3: *Data sources and response functions for forest trees.*

Tree species	**Beech and birch**	**Norway spruce**	**Deciduous oaks**	**Deciduous oaks**	**Evergreens**
Effect parameter	**Whole tree biomass**	**Whole tree biomass**	**Whole tree biomass**	**Root biomass**	**Above-ground biomass**
% reduction for critical level	4% (annual)	2% (annual)	4% (annual)	4% (annual)	4% (annual)
Critical level (POD_1SPEC, mmol m^{-2})	**5.2**	**9.2**	**14.0**	**10.3**	**47.3**
Biogeographical region*	B, C (A, S, P)	B, C (A, S, P)	M	M	M
Countries involved in experiments	Finland, Sweden, Switzerland	Sweden, Switzerland	Spain, Italy	Spain, Italy	Spain
Number of data points	34 (9 different experiments)	29 (8 different experiments)	10 (2 different experiments)	10 (2 different experiments)	22 (4 different experiments)
Years of experiments	1-5	1-4	2	2	1.5-3
Data sources	Braun and Flückiger, 1995; Büker et al., 2015; Karlsson et al., 2003; Oksanen, 2003; Uddling et al., 2004	Braun and Flückiger, 1995; Büker et al., 2015; Karlsson et al, 2004	Calatayud et al. 2011; Marzuoli et al. 2016 and in preparation	Calatayud et al. 2011; Marzuoli et al. 2016 and in preparation	Alonso et al., 2014 and in preparation ; Barnes et al., 2000; Calatayud et al., 2011; Inclán et al., 2005; Ribas et al., 2005
Time period	Growing season	Growing season	Growing season	Growing season	Growing season
Response function	RB(%) = 100.2 – 0.93 x POD_1SPEC	RB(%) = 99.8 – 0.22 x POD_1SPEC	RB(%) = 100.3 – 0.32 x POD_1SPEC	RB(%) = 100.6 – 0.45 x POD_1SPEC	RB(%) = 99.8 – 0.09 x POD_1SPEC
Adjusted R^2	0.67	0.31	0.41	0.48	0.42
P value	<0.001	<0.001	0.027	0.016	<0.001
Data curator (e-mail)	Patrick Büker (patrick.bueker@york.ac.uk)		Riccardo Marzuoli (riccardo.marzuoli@unicatt.it)		Rocio Alonso (rocio.alonso @ciemat.es)

** A = Atlantic; B = Boreal; C, = Continental, M = Mediterranean, S = Steppic, P = Pannonian. In brackets: not derived for those regions but could be applied there too.*

III.5.3.3 (SEMI-)NATURAL VEGETATION

Table A4 provides a summary of the data sources and O_3 flux-effect relationships for (semi-) natural vegetation as described in section III.3.5.4.

Table A4: *Data sources and response functions for (semi-)natural vegetation.*

O_3-sensitive species of:	**Temperate perennial grassland**	**Temperate perennial grassland**	**Temperate perennial grassland**	**Mediterranean annual pasture**	**Mediterranean annual pasture**
Representative species used to derive flux-effect relationship	*Campanula rotundifolia, Trifolium pratense, Sanguisorba major, Sanguisorba officinalis, Scabiosa columbaria, Fritillaria meleagris*	*Campanula rotundifolia, Dactylis glomerata, Leontodon hispidus, Ranunculus acris*	*Campanula rotundifolia, Primula veris, Potentilla erecta, Scabiosa columbaria*	*Trifolium striatum, T.cherleri, T.glomeratum, T.angustifolium, T.subterraneum, Medicago minima, Biserrula pelecinus*	*Trifolium striatum, T. cherleri, T. subterraneum*
Effect parameter	**Above-ground biomass**	**Total biomass**	**Flower number**	**Above-ground biomass**	**Seed/flower biomass**
% reduction for critical level	10%	10%	10%	10%	10%
Critical level (POD_1SPEC, mmol m^{-2})	**10.2**	**16.2**	**6.6**	**16.9**	**10.8**
Biogeographical regions*	A, B, C (S, P)	A, B, C (S, P)	A, B, C (S, P)	M	M
Countries involved in experiments	UK	UK	UK	Spain	Spain
Number of data points	47	53	32	51	15
Years of experiments	4	4	3	5	3
Data sources	Hayes et al., 2012; Hewitt et al., 2014; Hayes et al. unpublished	Wagg et al., 2012, Hayes et al., 2011, Wyness et al., 2011; Hayes et al., unpublished	Hayes et al., 2012; Hayes et al., 2011; Hayes et al. unpublished	Gimeno et al., 2004a; Sanz et al., 2005, 2007, 2014, 2016	Gimeno et al., 2004b; Sanz et al., 2007, 2016
Accumulation period	3 months	3 months	3 months	1.5 months	1.5 months
Time period for accumulation period	1 April to 30 Sept	1 April to 30 Sept	1 April to 30 Sept	1 February to 30 June	1 February to 30 June
Response function	RB(%) = 93.9 – 0.99 x POD_1SPEC	RB(%) = 94.7 – 0.62 x POD_1SPEC	RF(%) = 101.2 – 1.54 x POD_1SPEC	RB(%) = 97.1 - 0.85 x POD_1SPEC	RB(%) = 92.3 - 1.61 x POD_1SPEC
Adjusted R^2	0.10	0.34	0.30	0.57	0.59
P value	0.018	<0.001	<0.001	<0.001	<0.001
Data curator (e-mail)	Felicity Hayes (fhay@ceh.ac.uk)			Ignacio González-Fernández (ignacio.gonzalez@ciemat.es)	

** A = Atlantic; B = Boreal; C, = Continental, M = Mediterranean, S = Steppic, P = Pannonian. In brackets: not derived for those regions but could be applied there too.*

III.5.3.4 REFERENCES

Alonso, R., Elvira, S., González-Fernández, I., Calvete, H., García-Gómez, H., Bermejo, V., 2014. Drought stress does not protect *Quercus ilex* L. from ozone effects: results from a comparative study of two subspecies differing in ozone sensitivity. Plant Biology 16, 375-384.

Barnes, J.D., Gimeno, B.S., Davison, A.W., Dizengremel, P., Gerant, D., Bussotti, F., Velissariou, D., 2000. Air pollution impacts on pine forests in the Mediterranean basin. In: Ne'eman, G., Trabaud, L. (Eds.). Ecology, biogeography and management of *Pinus halepensis* and *P. Brutia* forest ecosystems in the Mediterranean basin. Leiden, The Netherlands: Backhuys Publishers, 391–404.

Braun, S., Flückiger, W., 1995. Effects of ambient ozone on seedlings of *Fagus sylvatica* L. and *Picea abies* (L.) Karst. New Phytologist 129**,** 33-44.

Büker, P., Feng, Z., Uddling, J., Briolat, A., Alonso, R., Braun, S., Elvira, S., Gerosa, G., Karlsson, P.E., Le Thiec, D., Marzuoli, R., Mills, G., Oksanen, E., Wieser, G., Wilkinson, M., Emberson, L.D., 2015. New flux based dose–response relationships for ozone for European forest tree species. Environmental Pollution 206, 163–174.

Calatayud, V., Cerveró, J., Calvo, E., García-Breijo, F.J., Reig-Armiñana, J., Sanz, M.J., 2011. Responses of evergreen and deciduous Quercus species to enhanced levels. Environmental Pollution 159, 55-63.

Gimeno B. S., Bermejo V., Sanz J., De La Torre D., Elvira S., 2004a. Growth response to ozone of annual species from Mediterranean pastures. Environmental Pollution, 132, 297–306.

Gimeno, B.S. Bermejo, V., Sanz, J., De la Torre, D., Gil, J.M., 2004b. Assessment of the effects of ozone exposure and plant competition on the reproductive ability of three therophytic clover species from Iberian pastures. Atmospheric Environment 38, 2295 – 2303.

González-Fernández, I., Calvo, E., Gerosa, G., Bermejo, V., Marzuoli, R., Calatayud, V., Alonso, R., 2014. Setting ozone critical levels for protecting horticultural Mediterranean crops: Case study of tomato. Environmental Pollution 185, 178-187.

Hayes, F., Mills, G., Harmens, H., Wyness, K., 2011. Within season and carry-over effects following exposure of grassland species mixtures to increasing background ozone. Environmental Pollution 159, 2420-2426.

Hayes, F., Williamson, J., Mills, G., 2012. Ozone pollution affects flower numbers and timing in a simulated BAP priority calcareous grassland community. Environmental Pollution 163, 40-47.

Hewitt, D.K.L., Mills, G., Hayes, F., Wilkinson, S., Davies, W., 2014. Highlighting the threat from current and near-future ozone pollution to clover in pasture. Environmental Pollution 189, 111-117.

Inclán, R., Gimeno, B.S., Dizengremel, P., Sánchez, M., 2005. Compensation processes of Aleppo pine (*Pinus halepensis* Mill.) to ozone exposure and drought stress. Environmental Pollution 137, 517-524.

Karlsson, P.E., Uddling, J., Braun, S., Broadmeadow, M., Elvira, S., Gimeno, B.S., Le Thiec, D., Oksanen, E., Vandermeiren, K., Wilkinson, M., Emberson, L., 2003. New Critical Levels for Ozone Impact on Trees Based on AOT40 and Leaf Cumulated Uptake of Ozone. In: Karlsson, P.E., Selldén, G., Pleijel, H., (Eds.). Establishing Ozone Critical Levels II. UNECE Workshop Report. IVL report B 1523.

Karlsson, P.E., Uddling, J., Braun, S., Broadmeadow, M., Elvira, S., Gimeno, B.S., Le Thiec, D., Oksanen, E., Vandermeiren, K., Wilkinson, M., Emberson, L., 2004. New critical levels for ozone effects on young trees based on AOT40 and simulated cumulative leaf uptake of ozone. Atmospheric Environment 38, 2283 - 2294.

Marzuoli, R., Monga, R., Finco, A., Gerosa, G., 2016. Biomass and physiological responses of *Quercus robur* (L.) young trees during 2 years of treatments with different levels of ozone and nitrogen wet deposition. Trees 30, 1995-2010.

Oksanen, E., 2003. Responses of selected birch (*Betula pendula* Roth) clones to ozone change over time. Plant, Cell and Environment 26, 875-886.

Piikki, K., De Temmerman, L. Ojanpera, K., Danielsson, H., Pleijel, H., 2008. The grain quality of spring wheat (*Triticum aestivum* L.) in relation to elevated ozone uptake and carbon dioxide exposure. European Journal of Agronomy 28, 245-254.

Pleijel, H., Danielsson, H., Emberson, L., Ashmore, M., Mills, G., 2007. Ozone risk assessment for agricultural crops in Europe: Further development of stomatal flux and flux–response relationships for European wheat and potato. Atmospheric Environment 4, 3022-3040.

Ribas, A., Peñuelas, J., Elvira, S., Gimeno, B.S., 2005. Ozone exposure induces the activation of leaf senescence-related processes and morphological and growth changes in seedlings of Mediterranean tree species. Environmental Pollution 134, 291-300.

Sanz, J., Bermejo, V., Gimeno, B.S., Elvira, S., Alonso, R. 2007. Ozone sensitivity of the Mediterranean terophyte *Trifolium striatum* is modulated by soil nitrogen content. Atmospheric Environment 41, 8952–8962.

Sanz, J., González-Fernández, I., Calvete-Sogo, H., Lin, J.S., Alonso, R., Muntifering, R., Bermejo, V., 2014. Ozone and nitrogen effects on yield and nutritive quality of the annual legume *Trifolium cherleri*. Atmospheric Environment 94,765–772.

Sanz, J., González-Fernández, I., Elvira, S., Muntifering, R., Alonso, R., Bermejo-Bermejo, V., 2016. Setting ozone critical levels for annual Mediterranean pasture species : Combined analysis of open-top chamber experiments. Science of the Total Environment 571, 670-679.

Sanz, J., Muntifering, R.B., Gimeno, B.S., Bermejo, V., Elvira, S., 2005. Ozone and increased nitrogen supply effects on the yield and nutritive quality of *Trifolium subterraneum*. Atmospheric Environment 39, 5899–5907.

Uddling, J., Günthardt-Goerg, M.S., Matyssek, R., Oksanen, E., Pleijel, H., Selldén, G., Karlsson, P.E., 2004. Biomass reduction of juvenile birch is more strongly related to stomatal uptake of ozone than to indices based on external exposure. Atmospheric Environment 38, 4709-4719

Wagg, S., Mills, G., Hayes, F., Wilkinson, S., Cooper, D., Davies, W.J., 2012. Reduced soil water availability did not protect two competing grassland species from the negative effects of increasing background ozone. Environmental Pollution 165, 91-99.

Wyness, K., Mills, G., Jones, L., Barnes, J.D., Jones, D.L., 2011. Enhanced nitrogen deposition exacerbates the negative effect of increasing background ozone in *Dactylis glomerata*, but not *Ranunculus acris*. Environmental Pollution 159, 2493-2499.